

AD-A064 440

MITRE CORP BEDFORD MASS

F/G 17/2.1

A SURVIVABLE NETWORK OF GROUND RELAYS FOR TACTICAL DATA COMMUNI--ETC(U)

DEC 78 S M SUSSMAN, L G DARIAN, K W RAU

F19628-78-C-0001

UNCLASSIFIED

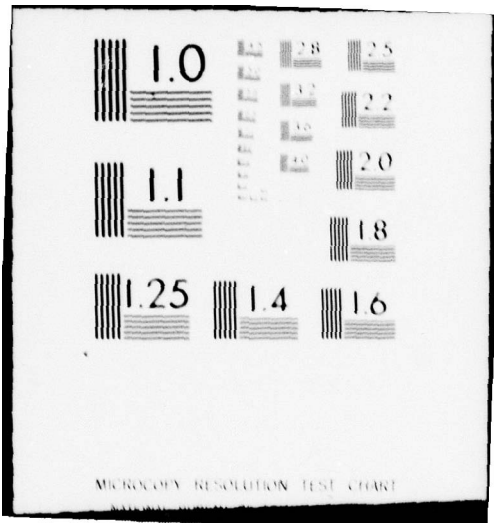
MTR-3647

ESD-TR-78-181

NL

1 of 2
AD
A064440





MICROCOPY RESOLUTION TEST CHART

LEVEL I

10
RWS

ESD-TR-78-181

MTR-3647

AD A 0 6 4 4 4 0

A SURVIVABLE NETWORK OF GROUND RELAYS
FOR TACTICAL DATA COMMUNICATION

BY S. M. SUSSMAN, L. G. DARIAN, AND K. W. RAU

DECEMBER 1978

Prepared for

DEPUTY FOR DEVELOPMENT PLANS
ELECTRONIC SYSTEMS DIVISION
AIR FORCE SYSTEMS COMMAND
UNITED STATES AIR FORCE
Hanscom Air Force Base, Massachusetts

DDC FILE COPY



DDC
RECEIVED
FEB 13 1979
E

Approved for public release;
distribution unlimited.

Project No. 666C
Prepared by
THE MITRE CORPORATION
Bedford, Massachusetts
Contract No. F19628-78-C-0001

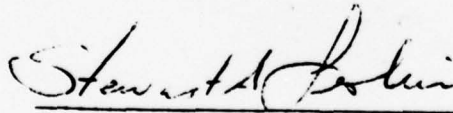
79 02 05 124

When U.S. Government drawings, specifications, or other data are used for any purpose other than a definitely related government procurement operation, the government thereby incurs no responsibility nor any obligation whatsoever; and the fact that the government may have formulated, furnished, or in any way supplied the said drawings, specifications, or other data is not to be regarded by implication or otherwise, as in any manner licensing the holder or any other person or corporation, or conveying any rights or permission to manufacture, use, or sell any patented invention that may in any way be related thereto.

Do not return this copy. Retain or destroy.

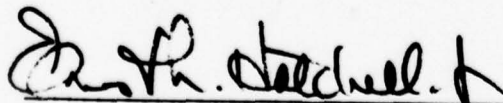
REVIEW AND APPROVAL

This technical report has been reviewed and is approved for publication.



Stewart A. Leshin, GS-13
Project Engineer

FOR THE COMMANDER



Ernest L. Hatchell Jr., Colonel, USAF
Assistant Deputy for Development Plans

UNCLASSIFIED

SECURITY CLASSIFICATION OF THIS PAGE (When Data Entered)

19 REPORT DOCUMENTATION PAGE		READ INSTRUCTIONS BEFORE COMPLETING FORM	
1. REPORT NUMBER 18 ESD-TR-78-181	2. GOVT ACCESSION NO.	3. RECIPIENT'S CATALOG NUMBER 9 Technical Reply	
4. TITLE (and Subtitle) 6 A SURVIVABLE NETWORK OF GROUND RELAYS FOR TACTICAL DATA COMMUNICATION		5. TYPE OF REPORT & PERIOD COVERED 14	
7. AUTHOR(s) 10 S. M. Sussman, K. W. Rau L. G. Darian		8. CONTRACT OR GRANT NUMBER(s) 15 F19628-78-C-0001	
9. PERFORMING ORGANIZATION NAME AND ADDRESS The MITRE Corporation P. O. Box 208 Bedford, MA 01730		10. PROGRAM ELEMENT, PROJECT, TASK AREA & WORK UNIT NUMBERS Project No. 666C	
11. CONTROLLING OFFICE NAME AND ADDRESS Deputy for Development Plans Electronic Systems Division, AFSC Hanscom AFB, MA 01731		12. REPORT DATE 11 DECEMBER 1978	13. NUMBER OF PAGES 115
14. MONITORING AGENCY NAME & ADDRESS (if different from Controlling Office) 12 117 p.		15. SECURITY CLASS. (of this report) UNCLASSIFIED	
15a. DECLASSIFICATION/DOWNGRADING SCHEDULE			
16. DISTRIBUTION STATEMENT (of this Report) Approved for public release; distribution unlimited.			
17. DISTRIBUTION STATEMENT (of the abstract entered in Block 20, if different from Report)			
18. SUPPLEMENTARY NOTES			
19. KEY WORDS (Continue on reverse side if necessary and identify by block number) ADAPTIVE MESSAGE ROUTING PACKET RADIO ANTI-JAM SPREAD-SPECTRUM CIRCULAR ARRAY SURVIVABLE RELAY NETWORK CODE-DIVISION MULTIPLE-ACCESS (over)			
20. ABSTRACT (Continue on reverse side if necessary and identify by block number) A concept and preliminary design parameters are presented for a multiple-connected network of ground-based data communication relays. Resistance to jamming is achieved by electronically steerable directive antennas with adaptive nulling and by spread-spectrum modulation. Adaptive store-and-forward routing (over)			

DD FORM 1 JAN 73 1473

EDITION OF 1 NOV 65 IS OBSOLETE

UNCLASSIFIED

SECURITY CLASSIFICATION OF THIS PAGE (When Data Entered)

235050

Handwritten signature or initials.

UNCLASSIFIED

SECURITY CLASSIFICATION OF THIS PAGE(When Data Entered)

19. KEY WORDS (concluded)

SWITCHABLE BEAM ANTENNAS
TACTICAL DATA COMMUNICATION

20. ABSTRACT (concluded)

provides protection against network disruption. A specific application is the information exchange among distributed tactical command and control facilities.

ACCESSION for	
NTIS	White Section <input checked="" type="checkbox"/>
DDC	Buff Section <input type="checkbox"/>
UNANNOUNCED	<input type="checkbox"/>
JUSTIFICATION	
BY	
DISTRIBUTION/AVAILABILITY CODES	
Dist.	AVAIL. / S. CIAL
A	

UNCLASSIFIED

SECURITY CLASSIFICATION OF THIS PAGE(When Data Entered)

ACKNOWLEDGMENTS

This report has been prepared by The MITRE Corporation under Project 666C. The contract is sponsored by the Electronic Systems Division, Air Force Systems Command, Hanscom Air Force Base, Massachusetts.

TABLE OF CONTENTS

	<u>Page</u>
LIST OF ILLUSTRATIONS	5
SECTION	
1 INTRODUCTION	7
1.1 SUMMARY	7
1.2 BASIC OBJECTIVE	10
1.3 SYSTEM OVERVIEW	11
1.3.1 Antenna Directivity and Its Implications	11
1.3.2 Channel Access	14
1.3.3 Adaptive Routing	16
2 PROPAGATION AND LINK POWER BUDGETS	17
2.1 PROPAGATION MODELS	17
2.2 SIGNAL-TO-JAMMER POWER BUDGET	18
2 2.3 SIGNAL-TO-NOISE POWER BUDGET	25
3 ANTENNA CONSIDERATIONS	27
3.1 ANTENNA REQUIREMENTS	27
3.1.1 Gain and Beamwidth	28
3.1.2 Sidelobes	32
3.1.3 Frequency/Bandwidth	34
3.1.4 Timing	35
3.1.5 Diversity	35
3.1.6 Dynamic Range/Power	36
3.2 ALTERNATE DESIGN APPROACHES	37
3.2.1 Phased Arrays	38
3.2.2 Lenses	39
3.2.3 Antenna Baseline Design	42
3.2.4 Baseline Design Variations	53

TABLE OF CONTENTS (concluded)

SECTION	<u>Page</u>
4 CHANNEL ACCESS, MODULATION AND SYNCHRONIZATION	55
4.1 CHANNEL ACCESS	55
4.2 SAW CONVOLVERS	59
4.3 DATA MODULATION	63
4.4 SYNCHRONIZATION	67
4.5 MODULATION PARAMETERS	70
4.6 NODE CONFIGURATION	71
4.7 NET ENTRY	73
5 MESSAGE ROUTING	77
5.1 DIRECTED MESSAGES	77
5.1.1 Routing Tables	77
5.1.2 Local Adaptation	78
5.1.3 Prior Message List	80
5.1.4 End-to-End Acknowledgment (ETE-ACK)	81
5.1.5 Flowchart	81
5.2 FLOOD ROUTING	81
5.3 GLOBAL PROGRAMMED ALGORITHMS	83
6 FUTURE WORK	84
APPENDIX A ADAPTIVE NULLING	85
REFERENCES	114

LIST OF ILLUSTRATIONS

<u>Figure Number</u>	<u>Page</u>
1.1 Directive Antennas	12
2.1 Multiple Jammer Geometry	24
3.1 Aperture Size as a Function of Frequency	30
3.2 Azimuth Beamwidth as a Function of Gain	31
3.3 Two-Dimensional Constrained Lens	40
3.4 Circular Array, Basic Beamforming	43
3.5 Receive Antenna Block Diagram	46
3.6 Column Printed Circuit Board - 48 Required	47
3.7 Beam Combiner Printed Circuit Board - 16 Required	48
3.8 Transmit Block Diagram	50
4.1 Packet Transfer Timing Diagram	58
4.2 Single Packet Transfer Timing Diagram	60
4.3 SAW Convolver	61
4.4 Effect of Delay Error	64
4.5 Four Orthogonal Waveforms	66
4.6 Node Block Diagram	72
5.1 Flowchart for Adaptive Routing Strategy	82
A.1 Sidelobe Canceller	86
A.2 Search Method	89
A.3 MSN Algorithm Representation	92
A.4 LMS Algorithm Representation	94
A.5 Array Dispersion	98
A.6 Convergence Response	101
A.7 Multiple Jammer Performance	103
A.8 Multiple Jammer Performance	104
A.9 Multiple Jammer Performance	105

LIST OF TABLES

<u>Table Number</u>	<u>Page</u>
2.1 Calculated Signal Attenuation Above Free Space Loss (dB)	19
2.2 Signal-to-Jammer Power Budget	21
2.3 Signal-to-Noise Power Budget	26
4.1 Modulation Parameters	69

SECTION 1

INTRODUCTION

1.1 SUMMARY

Effective operation of future Air Force Command and Control (C²) concepts will depend heavily on survivable communications among distributed C² facilities. For an advanced tactical communications system, survivability means the inclusion of features that will assure adequate capacity during hostilities ten or more years from now. When and where the system will be deployed is uncertain, nor can one predict the investment that an enemy may make to deny the use of the system. For these reasons the system described in this report is highly adaptable. It consists of redundant mobile elements which can be deployed in accordance with the intended use and the current threat. This paper presents the results of a preliminary investigation of one possible form of ground relay network to meet postulated requirements.

The concept of a multiple-connected relay network with adaptive routing and jamming resistance, based on spread-spectrum modulation and transmit/receive antenna directivity, promises to provide the essentials for survivable communications in support of tactical C² requirements. Other approaches are possible but no detailed comparative analyses have been conducted. Section 1.3 presents an overview of the ground relay network and introduces the major issues treated in more detail in the remainder of the report.

Propagation losses resulting from terrain effects are an important consideration in the design of a communication system to operate over "nonengineered" links, i.e., links where line-of-sight

(LOS) with adequate terrain clearance cannot be assured. Propagation data for a wide range of frequencies, link geometries, and terrain has been collected for mobile radio applications. In section 2.1 some of this data have been extracted to provide an input to the link power budgets. A representative value of 40 dB in excess of free space attenuation has been selected for the link calculations. This presumes that antennas are elevated above local foliage to avoid excessive attenuation at the candidate operating frequency of 7 GHz. The frequency was selected to provide the necessary gain with reasonable antenna sizes.

Sections 2.2 and 2.3 present power budgets for a postulated jamming threat and receiver noise, respectively. The S/J budget is based on an airborne jammer with direct LOS to the network receivers. Antenna directivity (47 dB transmit/receive gain product in favor of the desired signal) plus spread-spectrum processing gain (27 dB) provide an adequate antijamming (A/J) margin in spite of jammer transmitter power advantage (10 dB) and differential propagation loss (30 dB). Adequate noise margin is achieved with 200 watts transmitter power to communicate over 30 km at 400 kb/s raw data rate.

Antenna issues are discussed in section 3. The network concept is based on agile beam transmission and multiple beam reception, possibly with adaptive nulling. Several antenna design approaches are reviewed in section 3.2 and a candidate configuration consisting of a circular cylindrical array is described in detail. For one possible set of parameters (7 GHz, 5° azimuth, 10° elevation) the dimensions of the cylinder are approximately 1 ft in height and 2 ft in diameter. (Adaptive nulling is the subject of appendix A. The basic ideas are outlined, the pertinent performance factors are identified, and examples of achievable performance are cited.)

Topics related to channel access and spread-spectrum modulation are covered in section 4. Wideband pseudo-noise (PN) sequences (200 M chips/s) are the mechanism for A/J protection and spread spectrum or code division multiple access (CDMA). Each node operates in a half-duplex mode and can transmit to one neighboring node or receive from one or more neighbors. A contention scheme using a common PN code establishes a synchronized link prior to each message transfer; unique PN codes are employed for each transmitter-receiver pair during message transfer.

Data is conveyed by a quaternary alphabet of symbols each lasting $5 \mu\text{sec}$. The duration yields a time-bandwidth product of 1000 and is sufficient to avoid substantial intersymbol interference multipath delay. After allowing for channel utilization inefficiencies and half-duplex relay operation, the expected nodal throughput (one-half sum of inflow and outflow) is 100 kb/s. This number was selected as a reasonable target for a preliminary design.

Symbol detection and synchronization is based on surface acoustic wave (SAW) convolvers acting like matched filters for segments of a long PN sequence. Section 4.7 describes procedures for initial net entry of new nodes, including search through uncertainty regions in both time and azimuth angle.

Message routing protocols are discussed in section 5. Flood routing (all messages on all links) is a simple but perhaps inefficient broadcast protocol. Various other approaches for point-to-point and broadcast routing are possible. The main distinction between them is in the manner of calculating best routes, either (1) globally, by using known data on network connectivity or (2) locally, by extracting information from the headers of messages in transit. Of these two methods, the local optimization appears to respond more

rapidly to network changes. A specific local adaptation algorithm is described.

1.2 BASIC OBJECTIVE

The problem addressed in this report is to provide communications for the information exchange among distributed C² facilities. The key issue is system survivability with adequate communications capacity in the face of threats by weapons and jammers. Survivability against either threat is attained by means of redundancy and the capability for routing of traffic through the surviving connectivity. In a fluid combat environment, mobility is a major contributor to enhanced survivability. The communications support system must not become a limiting factor in the mobility of C² units. Hence, rapid redeployment and setup of the equipment is an essential feature of the tactical communication system.

The data flow in such a network would serve the needs of various tactical mission areas. The work reported here was initially undertaken to support the exchange of air tracks among netted short-range radars. Another application is the dissemination of friendly aircraft identification information to friendly air defense units, to minimize interrogation and/or radiation by both parties. Distribution of target data from intelligence collection and processing centers to weapon control points is also a potential source of traffic.

Any estimate of traffic load for a future tactical data network is subject to great uncertainty and will not be attempted here. Instead, a capacity goal of 100 kHz nodal throughput (one-half input rate plus output rate) has been selected for this preliminary network design. A capacity of this order of magnitude is consistent

with work reported elsewhere and appears to be within the reach of technology. Continuous feedback between requirements definition and technological capability is necessary to arrive at a workable cost-effective system design.

1.3 SYSTEM OVERVIEW

The proposed communications network has the general characteristics of multiple connectivity with adaptive routing, jam-resistance and low intercept susceptibility. Communication traffic, consisting of digital messages, will be conveyed by store-and-forward procedures through relay nodes, since ground-based C² facilities will often not be within reliable direct radio propagation range.

The expected jamming threat, particularly when emanating from dedicated airborne platforms, dictates a combination of spread-spectrum modulation and antenna directivity. A major feature of the proposed communication network is the use of steerable narrow-beam antennas to interconnect the nodes.

Figure 1.1 depicts several nodes with idealized antenna patterns and shows the various signal paths considered. The next three subsections introduce the main features of the proposed approach, followed by more detailed discussions in the remainder of the report.

1.3.1 Antenna Directivity and Its Implications

Since the network is not simply a chain of microwave repeaters, special procedures are required to establish connections between each node and its several neighbors. After initial startup, the

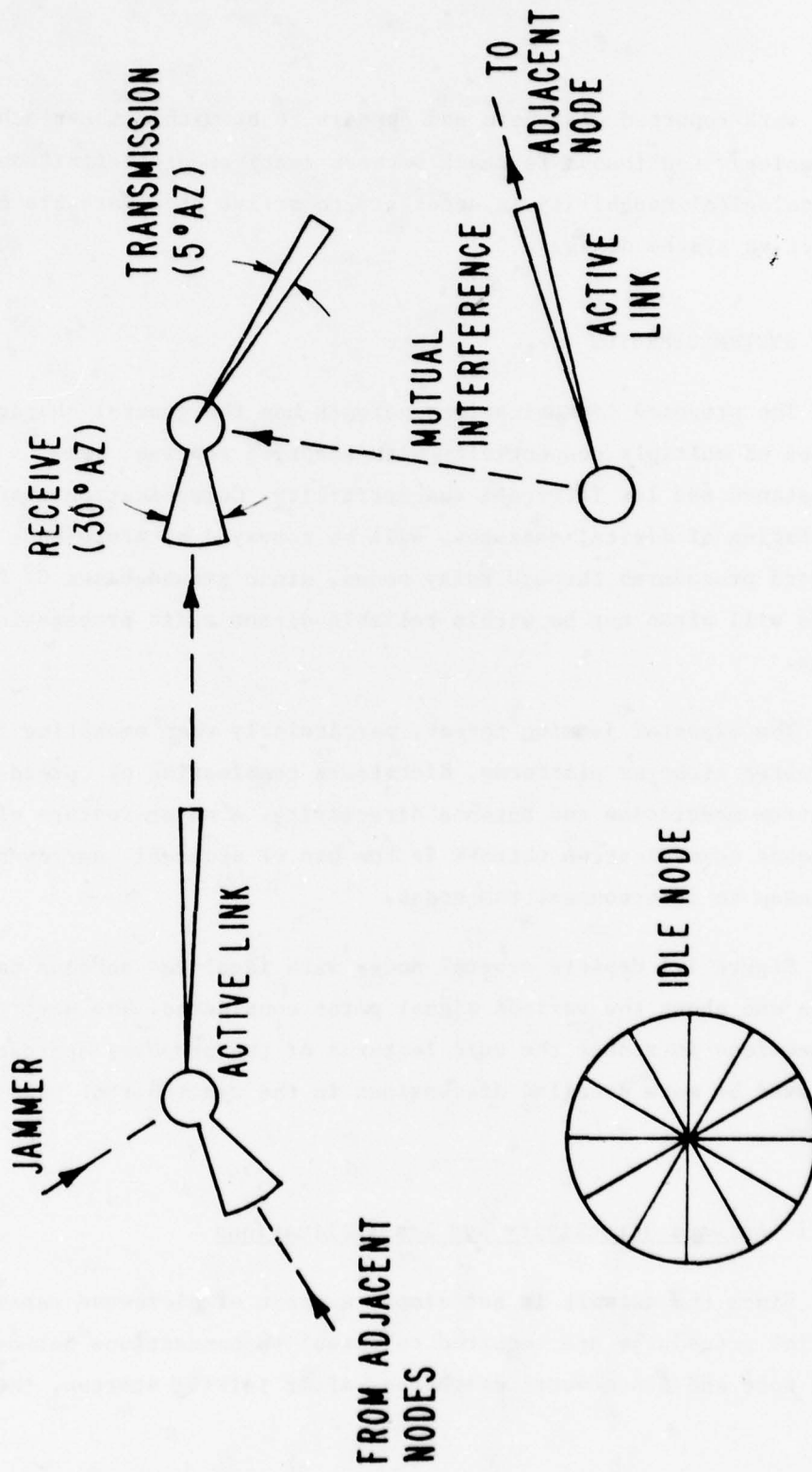


Figure 1.1 Directional Antennas

azimuth directions of all neighbors are stored at each node. When the need for a message transfer becomes known at both ends of the link, the respective beams can be steered or switched to the proper azimuth.

The node initiating the message transfer to a selected successor node can immediately transmit through a beam aimed at the intended receiver. The receiving node, however, has no prior indication as to which neighbor is attempting to establish a connection. Therefore, nodes must be capable of receiving from one of many possible directions, including not only the known neighbors but also the sites of new entries into the net. If reliable reception were possible in the face of noise, jamming, and mutual interference without azimuth directivity, a simple omnidirectional receiving antenna could be considered. The link budget calculations for the postulated conditions show that this is not the case. Substantial relative gain is required between desired signal direction and jammer or interfering sources. Moreover, since relay links may not have ideal LOS propagation, signal loss and noise considerations demand significant absolute gain in the receiving antenna.

These factors, which are treated quantitatively later on, lead to a possible receiving configuration consisting of a set of beams each with its own receiver and logic to detect valid signals. In figure 1.1 this concept is represented by the "Idle Node." The alternative of a scanning beam receiver, although less costly, would not only introduce excessive delay in link establishment but would also require the transmitter to radiate for a longer time while the receiver is searching.

The receiver achieves jammer and interference suppression through antenna directivity by one of two methods. The simpler approach relies only on the peak-to-sidelobe ratio of individual

directive antennas. Each antenna beam and associated signal processing is an independent receiving system. The second method strives to improve the jammer suppression by adaptive nulling, using the outputs of several directive antennas in combination. In effect, one or more of the antennas are used to cancel the jammer appearing in the main beam or sidelobes of the antenna aimed in the desired direction. The choice between the two approaches depends on the performance vs. complexity tradeoffs for adaptive nulling compared to achievable sidelobe levels in the individual antennas.

The above description of antenna characteristics suffices for this system overview. Section 3 includes further details on antennas, and section 4.7 discusses network entry procedures.

1.3.2 Channel Access

The channel access scheme considered here is based on the concept of spread-spectrum or code division multiple access (CDMA) techniques. The processing gain of the A/J spread-spectrum modulation also permits extraction of one of several overlapping communication signals, each employing a different pseudo-noise (PN) code. Message transfers on the relay links take place with a unique PN code for the specific node pair. Several message transfers involving different node pairs can proceed simultaneously in the same time-frequency space. Mutual interference is suppressed by a combination of propagation loss, antenna directivity, and processing gain. The last alone is inadequate to cope with the shared spectrum interference for unfavorable relative geometries. Without antenna directivity, a transmitter nearby the receiver could overwhelm the signal from a more distant node. The directive beams and receiving antenna nulling or low sidelobes assure with high probability that mutual interference passes through low-gain portions of the antenna

patterns at both ends of the interference path (see figure 1.1). Moreover, if restrictions are placed on the minimum distance between nodes, the network should not be subject to the "near-far" problem that is often a major obstacle to CDMA.

Each node has a single transmitter and multiple receivers. Simultaneous transmission and reception is not suggested because CDMA processing gain alone provides insufficient isolation from transmitter leakage. Message transfers occur on one outgoing link at a time from any node. As the connection is changed from one link to another, a protocol for code resynchronization and handshaking must be provided. This can be accomplished through a separate common code channel employed in a contention mode as follows.

A node in possession of a message to be transferred aims its transmit beam in the appropriate direction and transmits on the common code a request addressed to the desired neighbor. When not transmitting, all nodes listen on the multiple-receive beams with associated receivers. The receivers carry out a continual search to synchronize to the common code signal when it appears. The surface acoustic-wave (SAW) convolvers described later facilitate this process. After synchronization the request is decoded and, if the receiving node is the addressee, a reply is sent to the requestor. Since both ends of the link have been identified, the reply can be transmitted on the unique code for message transfer between the nodes in question, thereby freeing the common code channel for others. The requestor, anticipating a reply on the predetermined code, performs the appropriate synchronization search.

Long digital messages are segmented into packets, which are individually forwarded through the network to produce a "pipeline" effect, in that packets are relayed on the next hop before the entire message is received at the node. After both ends of the link

are synchronized, message transfer proceeds through a sequence of packet transmissions and hop-by-hop acknowledgments.

1.3.3 Adaptive Routing

An essential feature of a survivable communications system is the capability to reroute traffic around disrupted portions of the network. Moreover, in a highly mobile environment, nodes may be added or removed in response to user needs. Routing procedures should automatically respond to network changes to assure efficient utilization of existing connectivity and capacity. Two approaches may be considered. One is based on the shortest path algorithms of graph theory, and the other is an adaptive procedure using information carried by normal message traffic.

The shortest path algorithm for finding best routes from any one node to all others can be executed at each node, given a knowledge of network connectivity. Adaptation to network changes requires dissemination of connectivity data to all nodes. Dynamic behavior and alternate routing under the shortest path algorithm are unresolved issues.

The second approach employs a distributed algorithm for finding best paths, which does not require knowledge of total network connectivity at any node. Information on path length and quality is conveyed by messages in transit, allowing nodes to update routing tables. Partially random and alternate routing serves to find best paths adaptively as network changes occur. Questions regarding convergence and traffic congestion behavior of this algorithm remain to be answered.

SECTION 2

PROPAGATION AND LINK POWER BUDGETS

2.1 PROPAGATION MODELS

A ground-to-ground, survivable tactical communications network may not have the luxury of clear line-of-sight (LOS) propagation typical of well-engineered microwave relay links. Therefore, the influence of terrain is an important factor in the design and operation of the network. Unfortunately, the chief characteristic of radio propagation under these circumstances is its variability. Since theoretical treatments of propagation in complex terrain are generally intractable, empirical models have been created based on extensive measurements.

The most comprehensive model is the one evolved by Okumura (1). Compared to several others this model is found to be reasonably adequate. Okumura's model pertains to mobile radio communication at frequencies between 200 MHz and 3 GHz. The model is a series of graphical relationships for different terrain environments and link geometries. These combine to produce an estimate of the median propagation loss, defined as the attenuation between unity gain antennas. The propagation loss for distance d and frequency f comprises the free space loss.

$$L_{fs} = -32.45 - 20 \log f(\text{MHz}) - 20 \log d(\text{km})$$

and the additional attenuation due to terrain effects.

Application of the Okumura model requires definition of link parameters (frequency, distance, antenna heights), terrain

conditions (urban, suburban, open), and terminal location (local peak or trough). For conditions represented by a $\frac{1}{4}, \frac{3}{4}$ mix of open and suburban terrain respectively and terminals midway between peak and trough, Ormsby calculates median loss relative to free space for selected parameters. Table 2.1 presents the results; the different heights h (meters) are the same for both transmitter and receiver. The data for 5 GHz and for equal height terminals was obtained by extrapolation from Okumura.

It is interesting to note that there is little dependence on frequency. This behavior does not specifically include the effects of dense foliage near the terminals. A separate analysis showed that foliage attenuation is substantial and increases with frequency. For the frequencies considered (140 MHz to 1 GHz) the total loss was such that, for communication over practical distances, antennas would have to be elevated above the local foliage canopy. The power budget analyses assume that this is the case. In computing the signal-to-jammer ratios, we assume that the jammer is airborne and has a clear LOS to the receiver. The differential propagation loss for communicator and jammer consists of the distance ratio term in the free space loss and the terrain effect L_t represented by table 2.1. The differential loss is

$$L = L_s - L_j = 20 \log \frac{d_j}{d_s} + L_t.$$

For purposes of subsequent link analysis at 5 to 7 GHz, for distances 20 to 30 km with antenna heights 20 m or greater, L_t -40 dB is taken as a representative value.

2.2 SIGNAL-TO-JAMMER POWER BUDGET

Survivability in the face of jamming is a major objective of the proposed communications network. Therefore, the system

Table 2.1

CALCULATED SIGNAL ATTENUATION ABOVE FREE SPACE LOSS (dB)

f(MHz)	h = 3 m			h = 5 m			h = 15 m			h = 20 m		
	200	1000	5000	200	1000	5000	200	1000	5000	200	1000	5000
2	-52.5	-51.5	-52.5	-46.5	-45	-45.5	-27.5	-24.5	-23.5	-20.5	-17.5	-16.5
5	-57.5	-56.5	-59.5	-52.5	-51	-53.5	-33.5	-30.5	-31.5	-26.5	-23.5	-24.5
10	-61.5	-60.5	-63.5	-57.5	-56	-58.5	-39.5	-36.5	-37.5	-32.5	-29.5	-30.5
20	-64.5	-64.5	-67.5	-59.5	-59	-61.5	-42.5	-40.5	-41.5	-35.5	-33.5	-34.5
50	-76	-77	-82	-71	-71.5	-76	-54	-53	-56	-48	-47	-50
150	-80	-82	-89	-76	-77.5	-84	-57	-59	-66	-55	-55	-60

parameters were selected to cope with a postulated jamming threat. The S/J power budget developed in table 2.2 is the result of iterative attempts to reach a balance among the pertinent factors. To avoid fixing operating parameter values unnecessarily, where possible, the components of the S/J budget are expressed as ratios between communicator and jammer.

The SIGNAL column contains the parameter, either numeric or algebraic, for the link between communication transmitter and receiver. The JAMMER column gives the corresponding parameter, either numeric or relative to SIGNAL, for the link between jammer and communication receiver. The S/J column is the dB difference for each row, with positive numbers being favorable to the communication link. This method of expressing the signal-to-jammer power budget places in evidence the contribution of the various components to the total S/J. The total S/J is then compared to the minimum required value for the modulation and channel characteristics to determine whether the budget leads to satisfactory performance.

Consider first the single jammer case. In table 2.2, the transmitter power is treated in relative terms. If power P_T is available to the communicator, we assume that 10 dB more power can be generated by the jammer. This arbitrary ratio accounts for the possibly greater investment in each of a small number of airborne jammers compared to the large number of communication nodes. The transmit antenna gain for the communicator is taken to be 26 dB based on a 2 dB reduction from a peak gain of 28 dB. The assumed antenna has a beamwidth of 5° in azimuth and 10° in elevation. Further details on antenna characteristics are given in section 3.

The jammer's antenna directivity depends on the strategy pursued. Focussing jamming energy on a few selected nodes is unlikely

Table 2.2

SIGNAL-TO-JAMMER POWER BUDGET

	SIGNAL	JAMMER	SINGLE JAMMER S/J	MULTIPLE JAMMERS S/J
TRANSMITTER POWER	P_T	$P_T + 10$ dB	-10	-10
TRANSMIT ANTENNA GAIN (28 db PEAK)	+26	+12	+14	
FREE SPACE LOSS ($D_j = 3 D_c$)	Y	Y-10 dB	+10	+21
TERRAIN LOSS	-40	0	-40	-40
RECEIVE ANTENNA PEAK-NULLED OR SIDELobe RATIO			+33	+30
PROCESSING GAIN			+27	+27
		TOTAL S/J (E_b/N_{of})	+54 dB	+28 dB

to yield a payoff against an adaptive network. A single node may be defeated by a dedicated jammer, but the system should survive under broad-beam airborne jamming aimed at a large area of the network. For that threat the jammer's transmit antenna gain is 12 dB assuming an airborne platform with a sidelooking antenna pattern 100° in azimuth and 20° in elevation. For the relative S/J power budget in table 2.2 the operating frequency does not need to be defined. The frequency has a strong impact on antenna size and also influences the absolute propagation loss.

Free space loss is treated as a relative parameter. We assume that the ratio of jammer distance to communicator distance is around 3, leading to a 10 dB advantage to the communicator. A possible combination of distances under this assumption is a 25 km link and a jammer 75 km away.

Terrain loss in excess of free space loss is highly variable depending on antenna heights, distance, and type of terrain. As pointed out in section 2.1, a terrain loss of 40 dB represents a reasonable objective for the link power budget. The airborne jammer is assumed to have clear LOS to the victim receiver, and hence suffers no terrain loss.

The critical factor in the receive antenna pattern is the peak-to-null ratio, i.e., gain in the direction of the desired signal relative to gain toward the jammer. For either adaptive nulling or simply reliance on sidelobes, 33 dB is a reasonable number for the relative jammer suppression. (See section 3 and appendix A.)

The final entry in the S/J power budget is the processing gain derived from spectrum spreading. The processing gain is the ratio of the jammer bandwidth (assumed equal to the chip rate) and the raw transmission rate in bits/sec. The value of 27 dB is conservative

and consistent with the modulation scheme described in section 4. The total of S/J expressed as the ratio

$$\frac{E_o}{N_{Oj}} = \frac{\text{Energy per bit}}{\text{Jammer noise power density}}$$

is 34 dB for a single jammer.

The MULTIPLE JAMMERS column in table 2.2 was derived for the threat scenario depicted in figure 2.1. Flying parallel to the FEBA is a line of airborne jammers with characteristics the same as the single jammer. The distance between jammers is assumed to be the same as the closest distance to the communications receivers, viz., three times the distance between nodes. Under these circumstances, the total power at the receiver is readily computed taking into account the changing antenna gain due to different aspect angles and the varying distance to each jammer. The net effect is an increase of jammer power of 3 dB over the single jammer case. Therefore in table 2.2 the combined contribution of transmit antenna gain and free space loss is 21 dB. Terrain loss and processing gain are the same as for a single jammer. The peak-null ratio for the receive antenna is assumed to degrade by 3 dB when multiple jammers are present. The total E_b/N_{Oj} for the multiple jammer threat is 28 dB.

The S/J values of 28 to 34 dB are not excessive when one considers the signal fading phenomenon due to multipath propagation. For Rayleigh fading signals the bit error probability is on the order of 10^{-3} for the above E_b/N_o . If the receivers are implemented to capitalize on delay diversity, i.e., to combine the energy of resolvable multipath signals, a more favorable relation between error probability and E_b/N_o is achievable, and hence, the link budget tends to be conservative.

IA-51,738

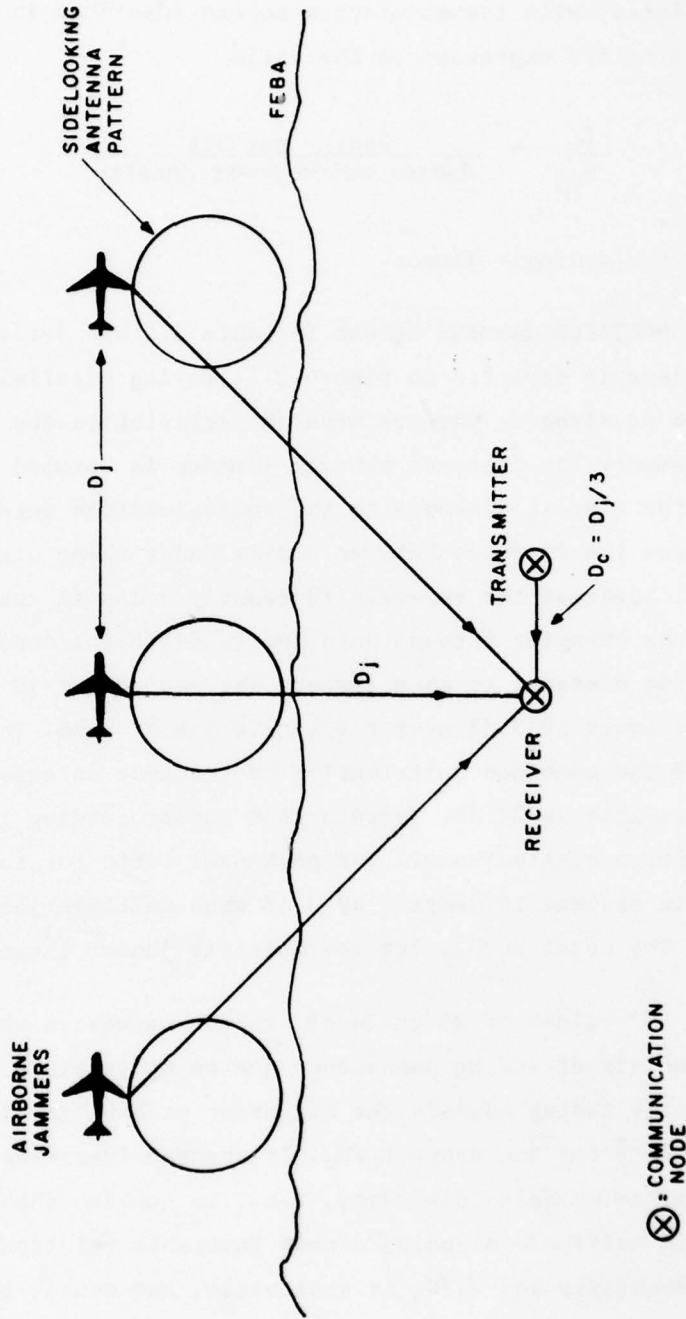


Figure 2.1 Multiple Jammer Geometry

2.3 SIGNAL-TO-NOISE POWER BUDGET

A communications system whose primary objective is jamming resistance must, of course, also function in a natural noise environment. At the frequency of interest for this application the dominant noise source is receiver thermal noise. Table 2.3 itemizes the signal-to-noise power budget.

In contrast to the S/J power budget, the operating frequency must now be defined. For the purposes of this preliminary analysis we have selected 7 GHz. This is high enough so that the antenna size for the required gain is within reasonable bounds and still low enough to avoid substantial atmospheric attenuation. Moreover, near 7 GHz the only allocation in a 250 MHz band seems to be for remote television pickups, which could easily coexist with the proposed system.

For reasons that will become clear in sections 3 and 4, the transmit and receive antenna patterns are asymmetric with peak gains of 28 dB and 20 dB respectively. The corresponding azimuth beamwidths are 5° and 30° assuming 10° width in elevation.

The S/N budget also requires that the signal power and data rate be defined. A 200 watts peak power referred to the antenna terminal is a reasonable minimum value to support the raw data rate of 400 kb/s (2.5 μsec bit time). The rationale for the latter is presented in section 4.5. The actual transmitter power may be larger than 200 watts in order to attain a desired A/J margin. The noise temperature of the receiving system also referred to the antenna port is assumed to be 1200°, i.e., 6 dB above reference noise. The remaining entries in the S/N budget of table 2.3 are the same as table 2.2 or are standard propagation loss components. The total E_b/N_0 is adequate, again taking into account the fading medium.

Table 2.3
SIGNAL-TO-NOISE POWER BUDGET

TRANSMITTER POWER (200 W)	+23	
TRANSMIT ANTENNA GAIN (28 dB PEAK)	+26	
PROPAGATION LOSS		
CONSTANT	-32	
20 LOG (30 km)	-30	
20 LOG (7000 MHz)	-77	
TERRAIN	-40	
RECEIVE ANTENNA GAIN (20 dB PEAK)	+18	
BIT TIME 2.5 μ SEC	+4	
		ENERGY/BIT
	-108	dBw μ sec
REFERENCE NOISE DENSITY (300° K)	-144	
SYSTEM NOISE TEMPERATURE (1200° K)	+6	
		NOISE POWER DENSITY
	-138	dBw/MHz
	+30	E_b/N_o dB

SECTION 3

ANTENNA CONSIDERATIONS

3.1 ANTENNA REQUIREMENTS

One of the main challenges in the realization of the proposed multiple-connected relay network is the implementation of a cost-effective antenna system to provide automatic steering of directive beams.

The primary constraints upon the antenna requirements are imposed by the benign link performance, as discussed in section 2.3. The transmit antenna gain and the receive antenna effective aperture, in conjunction with the other system parameters, must provide the required signal-to-noise ratio for the desired data rate and error rate. In addition, the antenna must provide spatial coverage and positioning consistent with the system connectivity, start up, and net entry procedures.

Additional requirements are imposed on the antenna by the system requirements for electronic survivability in a jamming environment, as discussed in section 2.2. Antenna parameters influenced by jamming survivability include the transmit gain and beamwidth, transmit and receive sidelobe levels, frequency of operation and bandwidth, beam shaping and steering, switching times, diversity, and dynamic range.

Specific antenna requirements must be derived in conjunction with the overall system evolution and cannot be defined independently. The following paragraphs indicate some of the tradeoffs involving the major parameters and the ways that system approaches

impact upon them. Some of the tradeoffs are implicit in the selection of parameters for the design examples in this report. However, a complete analysis remains to be performed.

3.1.1 Gain and Beamwidth

For the transmit antenna, gain should be maximized. This increases the effective isotropic radiated power (EIRP) and thus contributes directly to the system antijam margin. Since the region illuminated is limited, the probability of intercept and thus, jamming, is also reduced. The maximum transmit antenna gain is often bounded by the system scenario that requires coverage over a given region. Beyond this, the gain is limited by factors such as physical size and weight, or the impact of a narrow beam upon pointing accuracy, setup time, physical stability, the handshaking procedure, acquisition time, and so on.

In a benign environment, the required absolute gain for the receive antenna is only that necessary to meet link performance. In a jamming environment, however, the key to performance is the gain in the direction of the desired signal relative to the gain in the jammer direction. Relative gain improvement is most readily achieved by increased directivity. This is limited by the same factors cited for the transmit antenna. In addition, broader coverage is often required for receive functions to simplify and speed up acquisition of new participants in the net. Simultaneous receive connectivity to several users may also be necessary. This requires either broader beams (low gain) or multiple receivers.

For the postulated system, a two-way gain (logarithmic sum of transmit and receive gains) of about 50 dB is required. From the antenna viewpoint, the simplest and least expensive approach is to make the transmit and receive gains each equal to 1/2 of the total.

This permits the use of one aperture for both functions. For certain types of phased array or lens antennas, various options exist for using portions of the common aperture or beam combining to provide different gains from a common antenna. These are discussed in section 3.2.

Limits for unequal transmit/receive antenna gains can be determined by calculating the physical aperture required. To accommodate system requirements for setup without elevation steering, differences in terminal heights, and so on, an elevation beamwidth of 8° to 10° is required. Assuming this elevation beamwidth, figure 3.1 shows the physical aperture size required to achieve gains in the range of 15 to 35 dB as a function of frequency. It should be noted that this is the aperture size to provide a single beam. Thus the complete antenna system, which must be capable of beams in all directions, will be substantially larger, the precise amount being a function of the approach as discussed in section 3.2. These curves show that practical mobile antennas are limited to about 30 dB gain, and even then moderately high frequencies must be utilized.

Another constraint in determining the gain is the resultant beamwidth. For the assumed 8° to 10° elevation beamwidth, the variation of the azimuth beamwidth with gain is shown in figure 3.2. In the proposed system, the transmit beam must be stepped in azimuth to cover the entire 360° when entering the net. One hundred twenty (120) steps would be required for the 3° beam associated with 30 dB gain. This represents a reasonable upper limit for the scan cycle and thus also constrains the gain to 30 dB maximum. For 20 dB gain, the azimuth beamwidth is 30° . This substantially reduces the transmitter stepping problem. However, a 30° receive beam could receive several potentially interfering signals and has a higher probability of receiving a jammer within the main beam. Thus, it probably

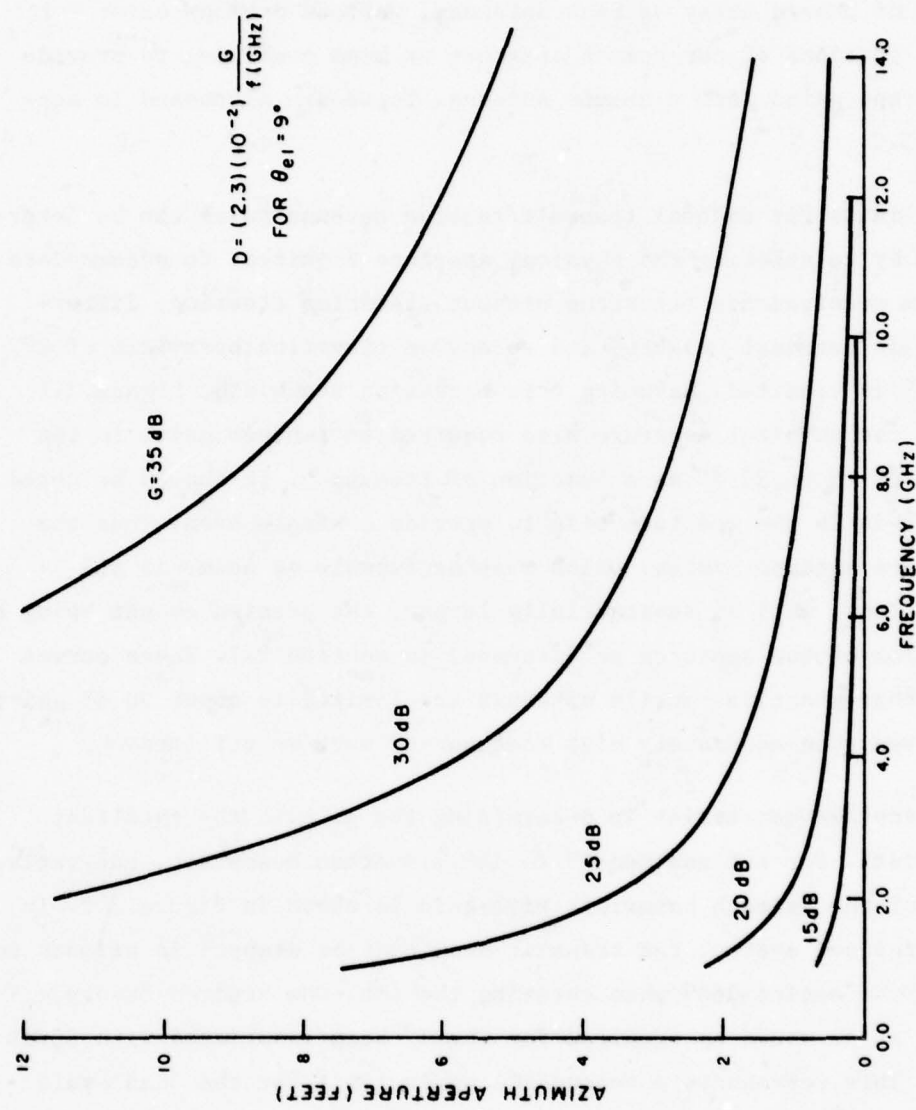


Figure 3.1 Aperture Size as a Function of Frequency

IA-51,528

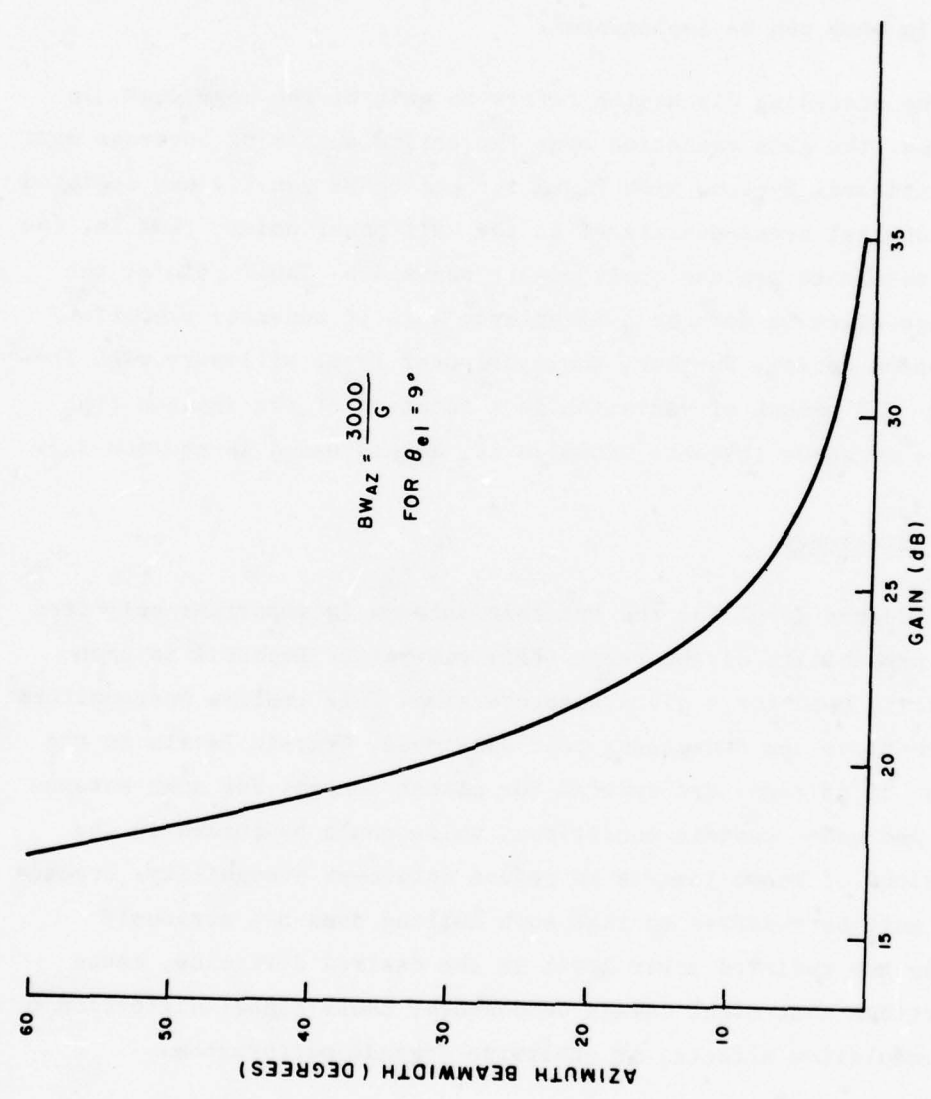


Figure 3.2 Azimuth Beamwidth as a Function of Gain

IA-91,536

represents a lower limit upon gain unless adaptive nulling within the main beam can be implemented.

The preceding discussion refers to gain at the beam peak. In practice, the gain variation over the entire sector of coverage must be considered. Systems with fixed stepped beams usually are designed for a nominal cross-over level at the half power point, that is, the step increments are one (half power) beamwidth. Thus, gain at the coverage edges is down by 3 dB or even more at moderate elevation/depression angles. Further, the cross-over level will vary with frequency. The amount of variation is a function of the antenna type and the measures taken to minimize it, as discussed in section 3.2.

3.1.2 Sidelobes

Sidelobe level for the transmit antenna is important only from a low probability of intercept (LPI) viewpoint. Emphasis is upon maximizing gain for a given aperture size. This implies near-uniform distributions and consequent poor sidelobes. Near-in levels in the -13 to -20 dB range are typical for planar arrays. For some antenna types and under certain conditions, nulls could be formed in the directions of known jammers to reduce intercept probability. Precautions must be observed so that such nulling does not seriously degrade the radiated power level in the desired direction, cause reflections that might damage components, cause signal distortion or intermodulation effects, or otherwise degrade performance.

For the receiver, suppression of jammer signals is of prime importance. Major performance and cost tradeoffs exist between overall low sidelobe design and generation of spatial nulls in the specific jammer directions through the various adaptive nulling techniques. The results of such a tradeoff are strong functions of

the particular antenna design, the magnitude of desired rejection, the number and location of jammers with respect to desired receive beams, and the specific methods of implementation. (See appendix A for an introduction to adaptive nulling and a survey of current capabilities.)

To achieve low sidelobes, the aperture distribution must be tapered. A larger physical aperture is then required to obtain the same beamwidth and gain. Increases of 40% or more, compared to uniform distribution, may be required for low sidelobes. In addition, stringent tolerances must be held on all factors affecting phase and amplitude. This includes rigid mechanical tolerances, precise transfer function tolerance, and low Voltage Standing Wave Ratio (VSWR) tolerances on all components. Such a design is subject to degradation due to physical damage, environment effects, improper field usage, and so on.

On the other hand, spatial nulling techniques may require auxiliary antennas, added components, extensive processing capability, and/or precision tolerances for some techniques. The adaptive array, however, is relatively insensitive to physical damage; it adapts to compensate for limited impairment.

For a design requiring a planar phased array, the addition of phase only, digital, adaptive nulling would have little impact on total system cost. For this type of system, 30 dB seems to be a break point between using low sidelobe design and adaptive nulling. A conclusion regarding the relative performance and cost merits, however, must be based upon an analysis of a specific design and cannot be generalized.

3.1.3 Frequency/Bandwidth

From the antenna cost viewpoint, higher frequencies are generally advantageous. As figure 3.1 shows, size decreases dramatically with frequency. This reduces antenna visibility, minimizes support structures (towers, masts, and so on), and generally decreases overall system weight. These advantages are offset to some extent by tighter tolerances and more difficult fabrication techniques. As frequency is increased, transmission line losses also increase. At some juncture, final transmitter components and receiver front ends must be collocated with the antenna, thus increasing the elevated weight. Costs of associated components such as solid-state transmitters, low noise front ends, circulators, and phase shifters tend to increase with increasing frequency while availability and many performance characteristics tend to degrade.

Perhaps one of the most important parameters in frequency selection is percent bandwidth. RF components tend to be frequency independent in terms of percent bandwidth. Thus at higher frequencies, wider frequency ranges are available for wideband techniques such as spread spectrum or frequency hopping. The system A/J margin can then be increased by using greater processing gain. If, on the other hand, the processing gain is held constant, the system performance will still improve due to the reduced percent bandwidth. Component performance will be improved, resulting in better basic link performance. The beamwidth change with frequency will be reduced resulting in smaller beam overlap changes. Even aperture and component frequency dispersion effects are reduced. This is critical for adaptive nulling techniques. As discussed in appendix A, nulling systems normally use phase weights rather than true time delay. Thus, a null is precisely positioned at only one frequency. At other frequencies, the null steers away from this point and the received

jammer signal is increased. The magnitude of this effect is a function of the bandwidth, the array size, and the null location with respect to array broadside.

Thus, there are distinct performance characteristic improvements associated with frequency increase/percent bandwidth reduction. All of the above considerations must be weighed in light of propagation characteristics (discussed in section 2) and other system parameters as well as allocation availability. Thus final frequency selection becomes a complex system tradeoff. The choice of 7 GHz for the design examples in this report is the result of a preliminary assessment of the competing issues.

3.1.4 Timing

Timing parameters generally are not critical from an RF viewpoint. Solid-state switches with nanosecond switching times are available and are compatible with most system approaches. At a system level, however, timing is one of the major issues, particularly as regards synchronization. (See section 4.4.) It is important to evolve and define timing requirements associated with entering the net and normal net operation. These impact heavily upon antenna parameters such as beamwidths, number of simultaneous beams, switching time between beams, dwell time per beam, and total time to scan a given coverage volume. Such parameters will influence the analysis and selection of an optimum antenna approach.

3.1.5 Diversity

The term diversity refers to a system characteristic by which two or more similar, but statistically uncorrelated, samples of the desired signal are combined. This can significantly reduce the

fraction of the time that the signal will drop down to an unusable level due to short-term fading. For microwave LOS systems, space diversity is most commonly used, although polarization, time, and frequency domains are also used. Several types of predetection and postdetection combining can be utilized, postdetection combining being the most common for digital systems. System level requirements for availability and propagation reliability must be established to determine the need for diversity and the resultant impact upon the antenna system.

For space diversity, two complete receive antenna systems would be required. For polarization diversity, considerable complication of feed or element design as well as isolation problems could result. Use of frequency diversity seems less likely for this application, but a form of inherent time diversity due to multipath delay spread may be possible as mentioned in section 4.

3.1.6 Dynamic Range/Power

The dynamic range of the receiver front end must be sufficient to accommodate both the low-level desired signal and a high-level jammer signal. RF components (phase shifters, attenuators, and so on) for adaptive null processing can also introduce dynamic range problems. In addition to possible saturation of the circuits themselves, the control signals used to adjust phase and amplitude are affected by the RF signal level and have dynamic range requirements of their own.

Power handling is not expected to be any problem in the antenna system. Reliable power generation could be accomplished with traveling wave tubes or solid-state devices. At the higher frequencies, multiple solid-state transmitters will be necessary to achieve

the total required power. This lends itself to a distributed transmitter in some form of phased array or lens antenna technique.

The use of a common transmit/receive aperture would require a T/R isolation device. This would take the form of a solid-state Single Pole Double Throw (SPDT) switch for a half-duplex system or a solid-state circulator for a full-duplex system.

3.2 ALTERNATE DESIGN APPROACHES

Many antenna design approaches can potentially satisfy the requirements for a network of multiple-connected microwave relays. These range from a relatively simple collection of mechanically steered dishes, to various types of lens structures or complex phased arrays. To determine the optimum approach, a baseline would have to be designed for each. Then, performance and cost tradeoff analyses would have to be performed considering the requirements of section 3.1 and any others imposed by the system design approach. Since the system design is still evolving, it is not fruitful to perform these designs and analyses at this time. Rather, a particular design that is reasonably flexible is postulated. This demonstrates one feasible approach and provides a departure point for either simpler or more complex approaches.

Some form of lens system or phased array is best suited to meet the requirements imposed by the system design. These approaches provide more flexibility and options for antenna parameter control in terms of beam shape, beam steering, multiple beam formation, switching speed, sidelobe control, adaptive nulling, and so on. The next sections briefly discuss some of the major considerations for these approaches.

3.2.1 Phased Arrays

For a phased array, the phasing is accomplished by two principal methods, true time and nontrue time (phase) delays. For true time delay, the transit time from the incident plane wave to the beam terminal is independent of the path taken through the feed or distribution network. Thus the array has broad instantaneous bandwidth and its beams do not steer with frequency. This is an important consideration for wideband antijam techniques and/or for adaptive nulling of broadband signals.

For nontrue time delay, the transit time from the incident plane wave to the beam terminal may vary by an integral number of RF periods. Element phasing for this method makes no distinction between a given phase, ϕ , and, $\phi + 2n\pi$, where n is an integer. Generally the phase shifters are limited in range from 0 to 360°. This results in shorter, smaller, and cheaper phase shifters than in true time delay. However, the resultant array is bandwidth limited by aperture dispersion effects and its beams steer with frequency change.

Multiple simultaneous receive beams can be achieved with phased arrays using either type of delay. The signal from each element must be divided, however, with an independent phasing network for each multiple beam. If fixed phasing networks are utilized, one must be provided for each beam position. For digital phase shifters, the number of networks can be reduced to the number of simultaneous beams, provided all beam positions are within the steering capability of the array.

Multiple simultaneous beams can also be provided by antennas such as a Blass Array or a Butler matrix. These, however, are not

true time delay systems and thus the beams steer with frequency. In addition, control of beam overlap, sidelobes, antenna nulling, and so on, is either more difficult or not possible.

3.2.2 Lenses

Other types of antennas that can produce high-gain, multiple beams and that are wideband by virtue of true time delay structures include spherical reflectors, Luneburg lenses, and constrained lenses. The choice depends on tradeoffs among many parameters. Because of its geometry, however, a constrained lens of the type shown in figure 3.3 provides considerable freedom and simplification in its component design and packaging. This lens was originally devised by Rotman (2) using Gent's (3) generalized equations for lenses of arbitrary shape. The lens is inherently broadband because it is based upon geometric optics, and all transmission components, such as parallel plates and coaxial lines, are TEM mode. High dielectric constant, low-loss dielectric material can be used in the parallel plate region to substantially reduce the size and weight of the lens.

Multiple beams are formed in the lens by locating multiple feeds/receivers at different points along the focal locus of the lens. Beam overlap as well as beam direction are controlled by positioning of the feed points. There is an option of switching between a full set of fixed beam ports or providing moveable beam ports.

Since the lens elements are coaxial cables, the aperture can take any configuration: planar, cylindrical, conformal, and so on. Because of the geometry, a common aperture is used for all beam positions, which results in efficient aperture utilization.

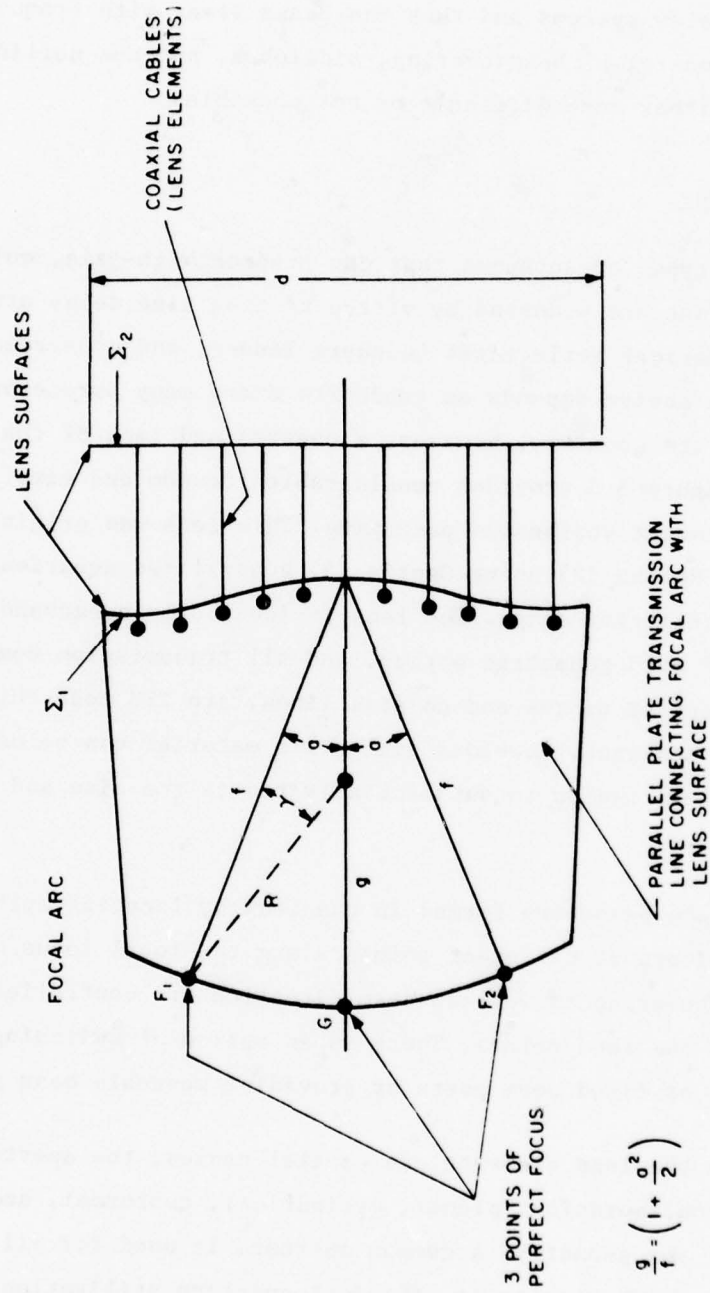


Figure 3.3 Two-Dimensional Constrained Lens

In such a multiple-beam lens design, the beam direction is frequency independent, that is, fixed in space. Because of the fixed aperture, however, the beamwidth will vary inversely with frequency and the cross-over level between adjacent beams will increase directly with frequency. These effects can be eliminated by the incorporation of frequency selective attenuators in the coaxial lens elements that feed the edges of the aperture. With proper design, the aperture distribution can vary with frequency so that constant beamwidth, pointing direction, cross-over level, and sidelobe level are maintained over frequency ranges exceeding an octave bandwidth.

It is also possible to use different segments of the focal arc for the primary feed. A large segment provides a narrow beam in the parallel plate region, illuminates a small portion of the lens surface, and produces a broad radiated beamwidth. Conversely, a small segment provides a broad beam in the parallel plate region, illuminates the total lens surface, and results in a narrow beamwidth. Thus, with proper design, it is possible to use differing segments to independently control beamwidth and gain for transmit/receive functions.

The design and evaluation of such a lens antenna are quite complex. Our purpose here is merely to show that an antenna design capable of supporting the system concept is feasible. A simpler phased array approach was selected and is described in the next section. This has no implications relative to the performance or cost advantages of lenses versus phased arrays. Such tradeoffs must be the subject of much more detailed design analysis and iterations of the system requirements.

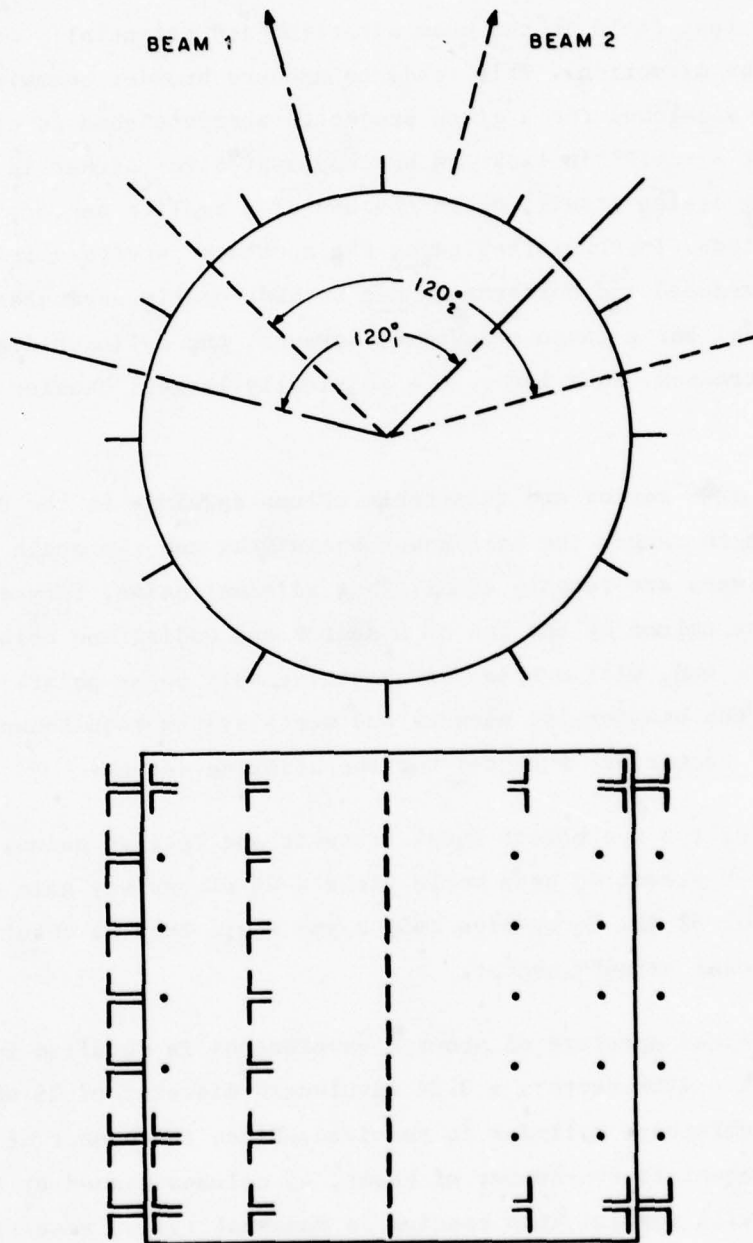
3.2.3 Antenna Baseline Design

The antenna baseline design is based upon the following assumptions concerning system parameters:

- a. Frequency of operation 7 GHz
Wavelength of operation 4.286 cm (1.687 in.).
- b. Two way gain greater than 50 dB.
- c. Single transmit beam, capable of positioning in any azimuth direction.
- d. Multiple simultaneous receive beams, capable of selecting any azimuth directions. Variable gain (i.e., azimuth beamwidth) up to that of the transmit beam is desirable.
- e. Sidelobe levels consistent with good antijam performance. The ability to add adaptive nulling is desirable.
- f. Elevation beamwidth 8° to 10° .

These requirements lend themselves to a cylindrical array design as shown in figure 3.4. Each vertical column of elements can be combined in a fixed manner to provide the desired elevation pattern characteristics. The columns within some sector of the cylinder are then combined to form a beam in the bisector direction (assuming nonscanning beamforming). Columns may be used for more than one beam direction as shown in figure 3.4.

The optimum sector size is also a complex tradeoff among several factors. The beamwidth is a function of the projected aperture of the sector. To minimize the physical size of the antenna required for a given beamwidth, the sector utilized should be as large as possible, the limit being 180° . Practically, however, very little aperture is gained beyond a 120° sector and the small increase is generally not worth the complexity of combining the additional columns. Additionally, each column has a radiation pattern whose



IA-51,537

Figure 3.4 Circular Array, Basic Beamforming

maximum is in a radial direction. Thus columns near the sector edge contribute less field in the beam direction and potentially more in the sidelobe directions. This tends to produce broader beamwidths and poorer sidelobes for a given projected aperture than an equivalent planar array. This lack can be compensated for either in the beamforming design itself, or in the use of a smaller sector, such as 90° or less. In the latter case, the aperture curvature is considerably reduced and performance can be made nearly equivalent to a planar array. For a given beamwidth, however, the cylinder diameter must be increased. This leads to a physically larger, heavier structure.

For a 120° sector and reasonable column spacings in the 0.5 to 0.6 wavelength range, the half power beamwidths and the angle between columns are roughly equal. Thus adjacent beams, formed by dropping one column at one end of a sector and adding one column at the opposite end, will overlap at about the half power point. This simplifies the beamforming network and meets system requirements. Thus a 120° sector was selected for the baseline design.

Assuming for the moment equal transmit and receive gains, an 8° azimuth by 8° elevation beam would yield a 26 dB one way gain or a total gain of 52 dB. Forty-five (45) beams would then be required to cover the total azimuth sector.

A projected aperture of about 8 wavelengths is required for the 8° beam. For a 120° sector, a 9.24 wavelength diameter or 29 wavelength circumference cylinder is required. Since the number of the columns is equal to the number of beams, 45 columns spaced at 0.645 wavelength will result. This spacing is somewhat large, resulting in real space, grating lobes being produced by the edge column pairs. This, in turn, would produce poor array sidelobes. Also, as will be

seen later, it is convenient to have the number of columns equal to a multiple of a binary number ($n2^m$ where n and m are integers). Thus 48 columns at 0.605 wavelength was selected for the baseline design. This spacing is still larger than the 0.557 wavelength theoretically needed to keep the grating lobes in imaginary space. It is estimated, however, that the grating lobe due to such spacing would be about 30 dB down from the main beam and thus acceptable. Further tradeoffs of size, column spacing, sector, sidelobe levels, and so on, would be the subject of a more detailed design. Sixteen (16) columns in a 120° sector are used to form a beam. To form the adjacent beam, the 120° sector is indexed one column, that is, one end column is dropped and one added at opposite ends. Thus each column is used in forming 16 beams.

A block diagram of the receive beam forming system is shown in figure 3.5 and some details of the implementation are shown in figures 3.6 and 3.7. Printed circuits are extensively used since they can be manufactured inexpensively. All boards shown are standard one layer microstrip design. In an actual design, multilayer stripline boards would be used since they would provide better performance and could present some manufacturing and/or packaging advantages.

Figure 3.6 shows a printed circuit board that would be used for a vertical column of elements. All others would be identical. As shown, the radiating elements are simple printed circuit dipoles about one-quarter wavelength above a ground plane. Twelve elements spaced about 0.7 wavelength apart will provide the elevation beamwidth. The elements are combined through a 12 to 1 weighted, printed circuit combiner. The weights can be adjusted to do some elevation pattern shaping and sidelobe control. Terrain effects, however, will be the primary determinant of in-the-field, elevation pattern performance.

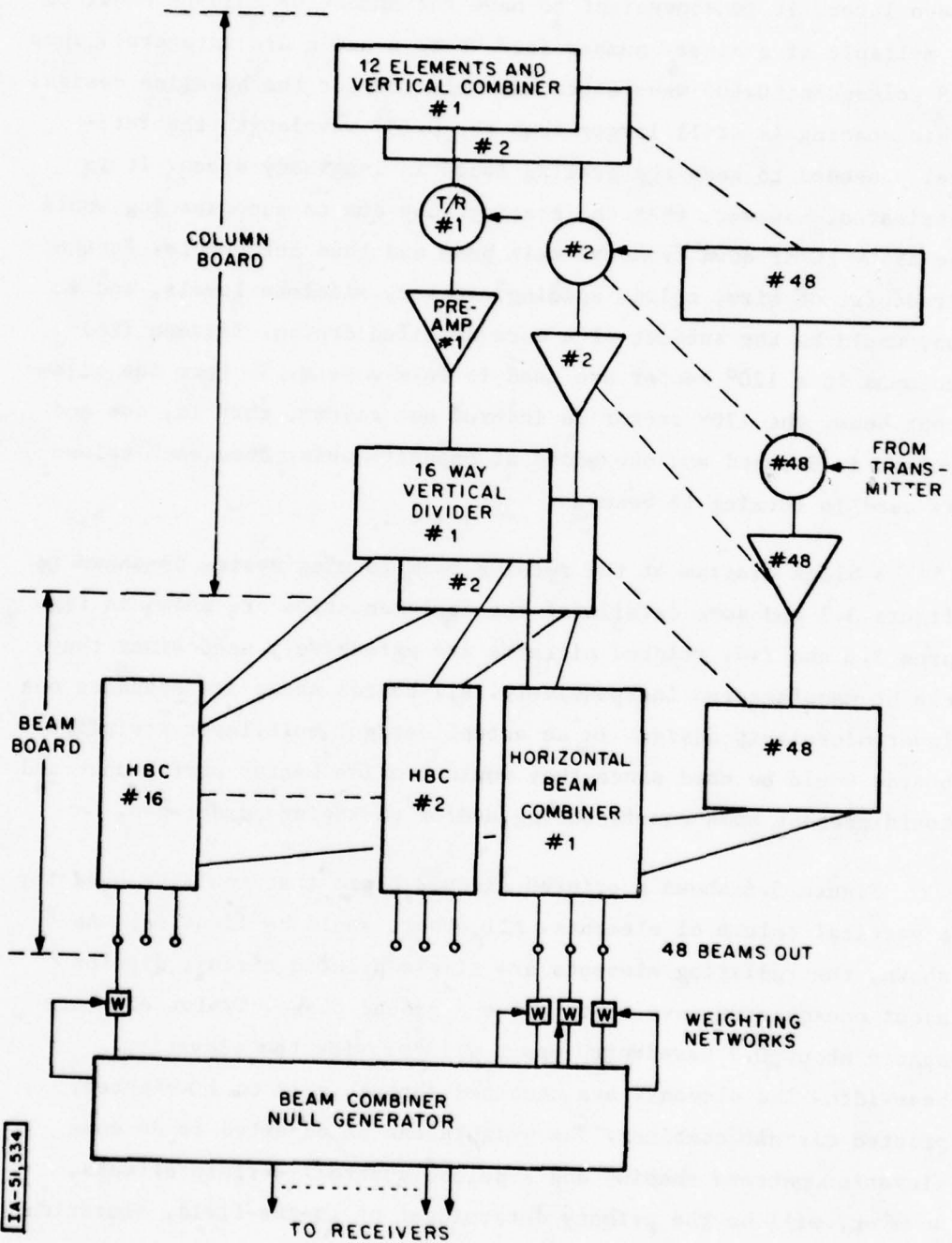
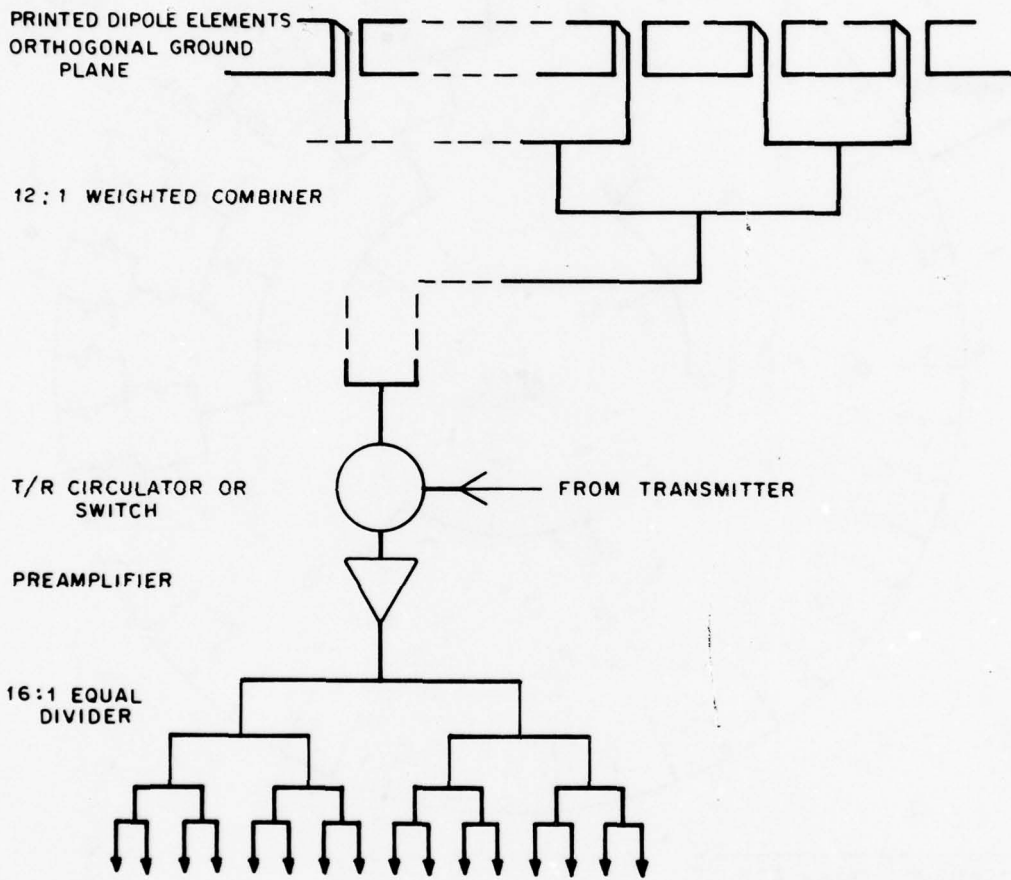


Figure 3.5 Receive Antenna Block Diagram



IA-91,531

Figure 3.6 Column Printed Circuit Board - 48 Required.

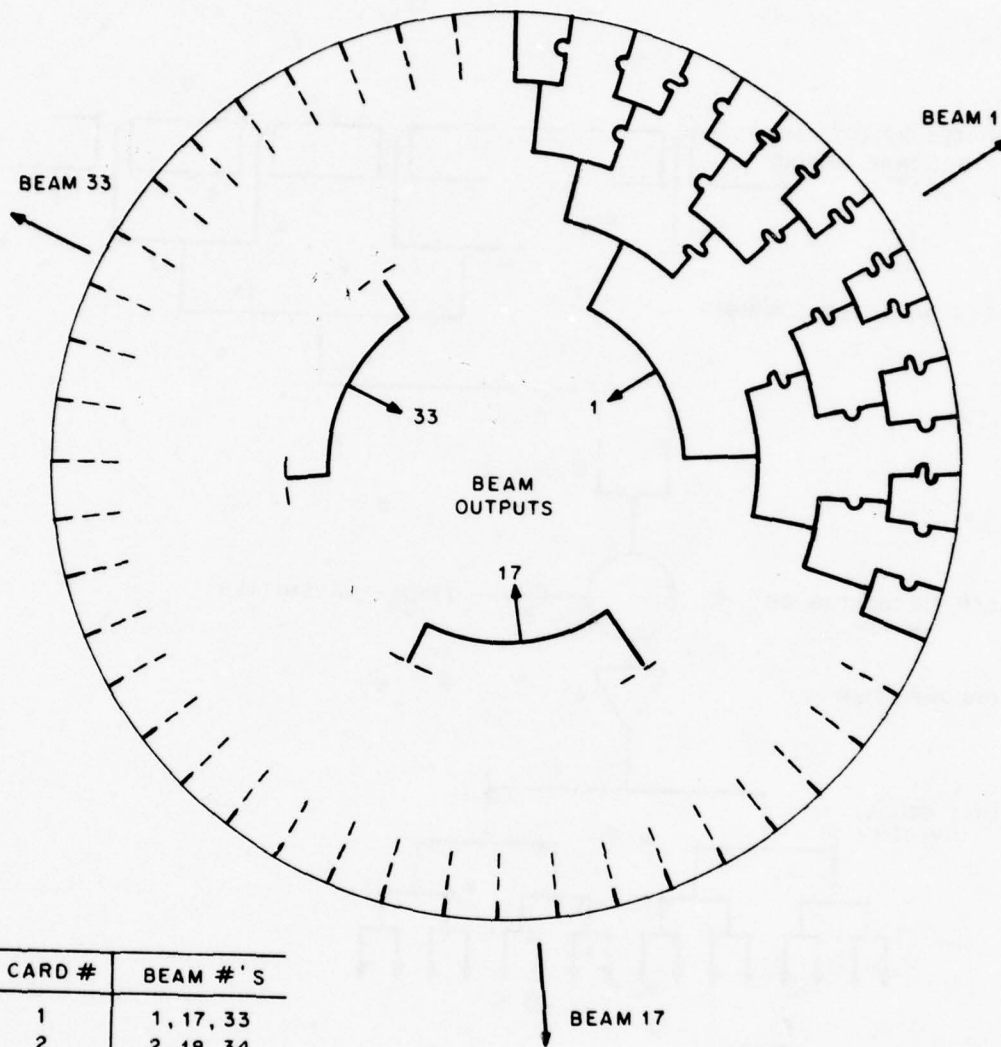


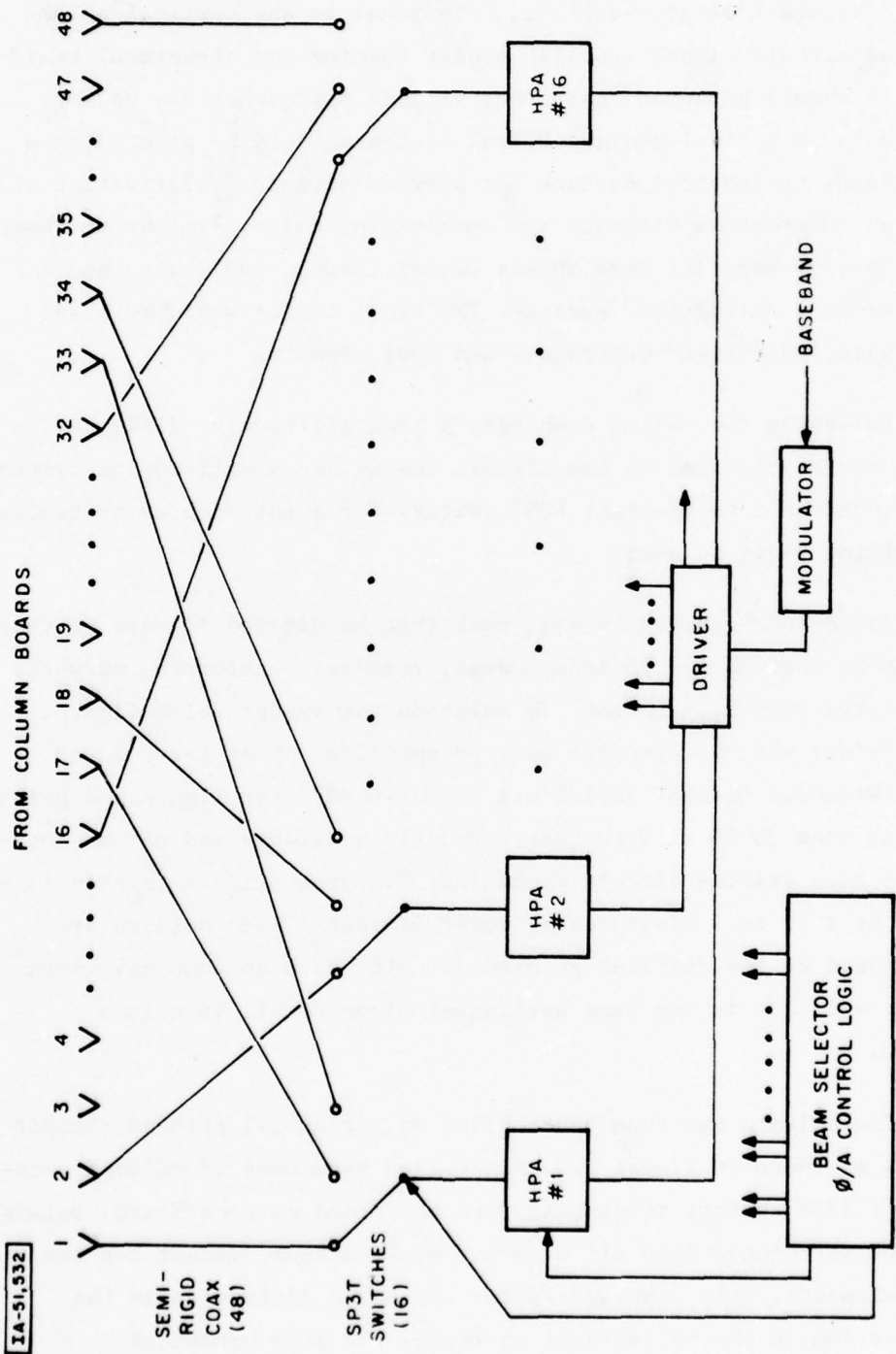
Figure 3.7 Beam Combiner Printed Circuit Board - 16 Required

A cylindrical ground plane, orthogonal to the vertical column printed circuit cards, provides proper spacing and structural rigidity. It should be noted that other element approaches may be more desirable in a final design. Spiral elements could be printed on a continuous cylindrical surface and provide circular polarization if desired. Microstrip elements and combiner circuits, similar to those developed by Rome Air Development Center (RADC), could also be printed on a cylindrical surface. The final choice would be based upon detailed design performance and cost results.

Following the column combiner, a transmit/receive (T/R) device would be incorporated in the circuit board. For a half-duplex system this could be a solid-state SPDT switch. For a full-duplex system, a circulator would be used.

The column received signal must then be divided 16 ways so that it can be used in the 16 independent, receive, beamforming networks associated with each column. To maintain the system noise figure, the divider must be preceded by a preamplifier of at least 12 dB gain. Wideband GaAsFET amplifiers with 4.0 dB noise figure and gains greater than 20 dB at 7 GHz are currently available and can be integrated into printed circuit packaging. The preamplifier is then followed by a 16 to 1 binary equal power divider. These outputs are positioned on the vertical printed circuit board so that any given output will lie in the same horizontal plane on all 16 column bounds.

The columns can then be combined on horizontal printed circuit boards as shown in figure 3.7. Since each beam uses 16 columns occupying a 120° sector, three beams can be formed on each board. Delays must be introduced into all elements of each beam, except for the edge elements. This compensates for the phase difference in the columns due to the cylindrical aperture. For best bandwidth



IA-51,532

SEMI-RIGID COAX (48)

SP3T SWITCHES (16)

HPA #16

HPA #2

HPA #1

DRIVER

MODULATOR

BASEBAND

FROM COLUMN BOARDS

1 2 3 4 . . . 16 17 18 19 . . . 32 33 34 35 . . . 47 48

Figure 3.8 Transmit Block Diagram

performance, these should be true time delay. Amplitude taper can also be introduced in the combiner, either by attenuation or unequal combining, to yield better receive sidelobes.

The three beam outputs on each board correspond to beams located 120° apart. Each board is indexed one column with respect to its neighbor, providing the 48 beam outputs from the 16 boards as shown in figure 3.5. These 48 outputs correspond to 48 receive beams, approximately 8° half power beamwidth, located 7.5° apart in azimuth. Multiple receivers could be connected to these outputs by a switch matrix.

Alternatively, beam outputs can be combined to effectively yield a broader beam for a given receiver. In the limit, progressively phasing each beam by its 7.5° spatial separation will yield an omnidirectional pattern for one receiver. In each case of broader beams, however, the receive gain is reduced in proportion to the azimuth broadening.

Finally, an adaptive nulling system with beam weighing could be used to generate nulls in the direction of interfering signals as shown in figure 3.5. (See also appendix A.) In the simplest form, unused beams could be used as sidelobe suppression elements to cancel any jammer within their coverage. Other more complex techniques might provide better performance and would have to be analyzed.

It may also be possible to perform adaptive weighing at the column level. Performing it at the beam level, as shown, permits growth potential and/or operational flexibility since the array can operate with or without the nulling system as required.

The transmit beamforming/switching system is shown in figure 3.8. From the T/R devices, 48 semirigid coaxial cables would run to

16 SP3T switches as shown. Control of these switches would select the proper 16 adjacent columns to form a beam in the desired direction.

The 16 columns are driven by 16 final power amplifiers that are in turn driven by a common driver stage. For the 200 W total power, this still exceeds the capability of current, single, solid state devices at 7 GHz. Thus hybrid combinations of solid-state devices or traveling wave tubes would be utilized.

Phase control would be required to compensate for aperture curvature as in the receive case. Amplitude control could also be used to control sidelobes at the expense of reduced gain. Knowledge of jammer directions from the receivers could be used to generate nulls in those directions (as long as they were outside the main beam) and thus reduce probability of intercept and possibly cause shutdown of look-through jammers.

This baseline design meets all the requirements identified at the beginning of this section. Multiple simultaneous, $8^\circ \times 8^\circ$ receive beams, limited only by the number of receivers, can be formed in independent azimuth directions. Variable receive azimuth beamwidths from 8° to 360° with corresponding gains of 26 dB to about 10 dB can be provided by appropriate beam combining. Adaptive nulling can be built in or added at a later date as needed. A single, $8^\circ \times 8^\circ$ transmit beam, capable of positioning in any azimuth direction, is provided. Nulling in jammer directions for the transmitter can also be provided if receive nulling is implemented. Physically, the antenna is a cylinder only 41 cm (16 in.) in diameter and 36 cm (14 in.) high. Parts of the transmitter and receiver, particularly the power amplifiers, will be external to that envelope and add considerable volume.

This baseline design is very similar to a cylindrical array developed independently by Lincoln Laboratory for short-range radar applications. Some pattern calculations and measurements, using a 30 dB Taylor distribution for sidelobe control, have been made by Lincoln. Such calculations and the cylindrical array design are complicated by the radial nature of the column patterns. The column amplitude weighting must be adjusted to account for the differences in column pattern magnitude in the desired array beam direction. Using estimated column patterns, Lincoln designed and built a distribution network that would yield the desired 30 dB Taylor taper. Array patterns with near-in sidelobes of -23 dB decreasing to about -35 dB relative to peak were measured. It was determined that the pattern of the column embedded in the array differed considerably from the estimated pattern. If this actual pattern, rather than the estimated one, had been used to determine column weighting, a -28 dB, near-in, sidelobe level would probably be achieved. The overall array and beamforming techniques used by Lincoln are very similar to the baseline design presented here and, hence, confirm its feasibility.

3.2.4 Baseline Design Variations

As discussed in section 3.2.3, a final design could use a smaller sector. This could provide improved sidelobes. Crossover levels would be higher and more beams would be required until about a 60° sector is reached. At this point, two columns can be dropped and added for each beam step. No basic changes in the design, other than column weighting and overall antenna size, are required to use a different sector. For example, a 90° sector would still use 16 columns. Each column would still be divided 16 ways. Each horizontal beamforming board would now contain 4 beams for a total of 64 beam outputs. The transmitter switch matrix would require SP4T switches,

otherwise the transmitter is identical. The cylinder diameter would be increased by the use of smaller sectors. For 90° sectors it would be about 48 cm (19 in.) and for 60° sectors, 69 cm (27 in.), both reasonable for a mobile system. The 90° sector array would contain 64 columns total and the 60° sector array would contain 96 columns total.

Unequal transmit and receive beams can also be provided by this design, since independent beamforming networks are used. For example, a 60° sector could be used for receive functions. This would provide lower gain and better control of sidelobes. (A reasonable number of columns must be included in the receive sector or the ability to control sidelobes will be lost.) A 120° sector could be used for transmit functions. This would provide the required gain with a minimum antenna physical size at the expense of sidelobes. A wide range of tradeoffs among gain, sidelobes, physical size, and so on, are available for a final design.

This design approach is best suited to transmit/receive beamwidths that differ by a maximum ratio of about 3. A design consistent with the 5° transmit beamwidth and 30° receive beamwidth postulated in section 2 can be accommodated, however. Assuming a 120° sector for transmit, approximately a 12-wavelength aperture is needed, resulting in a 14-wavelength or 60 cm (24 in.) diameter cylinder. The receive aperture need be only 2-1/2 wavelengths or a 20° sector. The principal difficulty with this design would be that only 5 columns are used for the receive beam. Thus, achieving good receive sidelobes and consequent good A/J protection without adaptive nulling would be difficult.

SECTION 4

CHANNEL ACCESS, MODULATION AND SYNCHRONIZATION

4.1 CHANNEL ACCESS

The link signal design presented in this section is based on the spread-spectrum code-division multiple access (CDMA) concept using a shared frequency band for all links. The multiplex alternatives of frequency division (FDM) or assigned time division (TDM) have not been explored in great depth, but appear to lead to considerable inefficiencies in spectrum or time occupancy. Both FDM and TDM would pose formidable channel allocation (net management) problems, especially since each node must support several links in different directions either in parallel (FDM) or in sequence (TDM). Moreover, mobility requirements demand that the link connectivity, i.e., neighboring nodes, be changed at more or less frequent intervals. Without FDM, simultaneous transmission and reception is not feasible; hence each node operates in a half-duplex mode. Spread-spectrum modulation by pseudo-noise (PN) rather than by frequency hopping has been chosen for this conceptual design primarily because PN has more favorable Low-Probability-of-Intercept (LPI) characteristics and is not susceptible to frequency-following jammers. In a future, more detailed design study, it would be desirable to revisit the signal design issue and to perform comparative evaluations of several candidates.

The basic idea for channel access is a contention scheme in a common PN code channel to establish a connection, with message transfer following in a unique CDMA channel. The contention scheme is based on the ALOHA concept (4), i.e., a low-duty-cycle

uncoordinated TDM format of data packet transmission. A necessary condition for successful reception is the absence of "collisions" among contending packets. Alternative methods of carrier sensing before transmission were briefly considered but do not appear attractive for the following reasons:

1. Due to propagation limitations, the transmitter cannot ascertain the signal environment of the intended receiver. This produces a phenomenon termed "the hidden terminal problem," which means that the transmitter is unable to sense a signal source that would interfere with its own transmission at the receiving site. In the suggested deployment of nodes, this condition would prevail frequently.
2. To take advantage of carrier sensing, potential transmission start times have to occur at intervals shorter than packet durations. Otherwise, sensing the channel is redundant because it will be clear for new users at the next start time anyway. A conflicting requirement, arising from synchronization considerations, is for the transmission start times to be separated by more than the time uncertainty between nodes. Procedures for link synchronization are described in section 4.4.
3. For spread-spectrum A/J modulation, sensing of channel occupancy by energy detection may fail or be subject to spoofing, while sensing by means of the code will entail a search lasting at least as long as the time uncertainty.

In the ALOHA contention channel the information to be conveyed per slot is minimal. To establish a connection for a message transfer to a specific neighbor, a node sends on the order of 32 bits consisting of a preamble to recognize the start-of-transmission (5 bits), message type (3 bits), addressee (12 bits) and sender (12 bits). The reply is transmitted via the predetermined unique code for the node pair. The sender and addressee are automatically identified through the code, hence the reply need only contain a few bits of information and may, in fact, be simply an acknowledgment.

The exchange of request and reply allows both ends of the link to synchronize code generators to the respective received signals. Thereafter, message transfer takes place through a sequence of packet transmissions and hop acknowledgments. The message is presumed to be segmented into several packets whose size remains to be determined. For reasons of efficiency that will become clear shortly, the packet duration should be longer than the maximum round-trip delay for any link.

A timing diagram is shown in figure 4.1 for the transfer of a message comprising three packets labeled 1.1, 1.2, 1.3. The vertical dimension represents time (increasing downward) at three nodes A, B, and C. The diagonal strokes denote propagation delay between nodes. A transmission period is marked by a heavy vertical bar on the time axis. The corresponding reception intervals are represented by the absence of a bar on the receiving node's time axis. Use of the contention channel is indicated by the shaded propagation intervals. Other intervals employ the unique code. Hop-by-hop acknowledgment (ACK) is shown as a reverse transmission of the same length as the reply to the connection request. We observe that the indicated overlap of ACK reception and packet reception implies a dual receiver capability. Also note that next packet transmission does not immediately follow receipt of ACK. Rather, the spacing between successive packets of the same message is fixed so as to allow the successor node sufficient time to acknowledge and forward a packet. Note that if packets were shorter than the round-trip delay, the forwarding node would be idle part of the time.

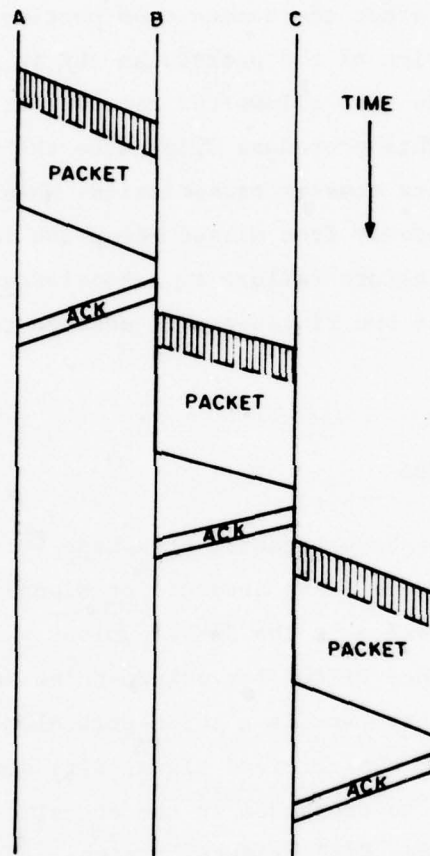
The diagram implies very fast processing to generate ACKs; if this proves troublesome, transmission of ACK can lag by one cycle. Missed packets are then inserted later in the sequence.

When messages are short enough to fit into one packet, it is possible to save time by sending the packet directly following the request. The transmission shifts from contention channel code to the unique code without the intervening reply. The receiver makes a corresponding shift after the common code portion is interpreted. Upon successful reception of the packet, an ACK is issued using a segment of the unique code that allows the receiver to synchronize and detect the ACK. This procedure eliminates the handshaking and synchronization before message transmission. When successful, it saves time, but its recovery from missed reception is longer since more time must elapse before failure to acknowledge can be determined. A timing diagram for the single-packet message transfer is shown in figure 4.2.

4.2 SAW CONVOLVERS

Great strides have recently been made in the development of surface-acoustic-wave (SAW) devices for signal processing applications. One such device is the SAW convolver which can implement a programmable matched filter for pseudo-noise sequences. In functional form the convolver is a three-port element as shown in figure 4.3. The input for the received signal $S(t)$ drives a transducer that causes the signal to propagate in the acoustic medium. A similar port for a reference $R(t)$ produces a signal that propagates in the opposite direction. Within the medium there is a nonlinear interaction region where the two signals are multiplied and integrated over the length of the region. The third port is the output $V(t)$ in the form of the convolution between signal and reference:

$$V(t) = \int_0^T S(t-\tau) R(t-T+\tau) d\tau,$$



IA-51,330

CONTENTION

Figure 4.2 Single Packet Transfer Timing Diagram

IA-91,930

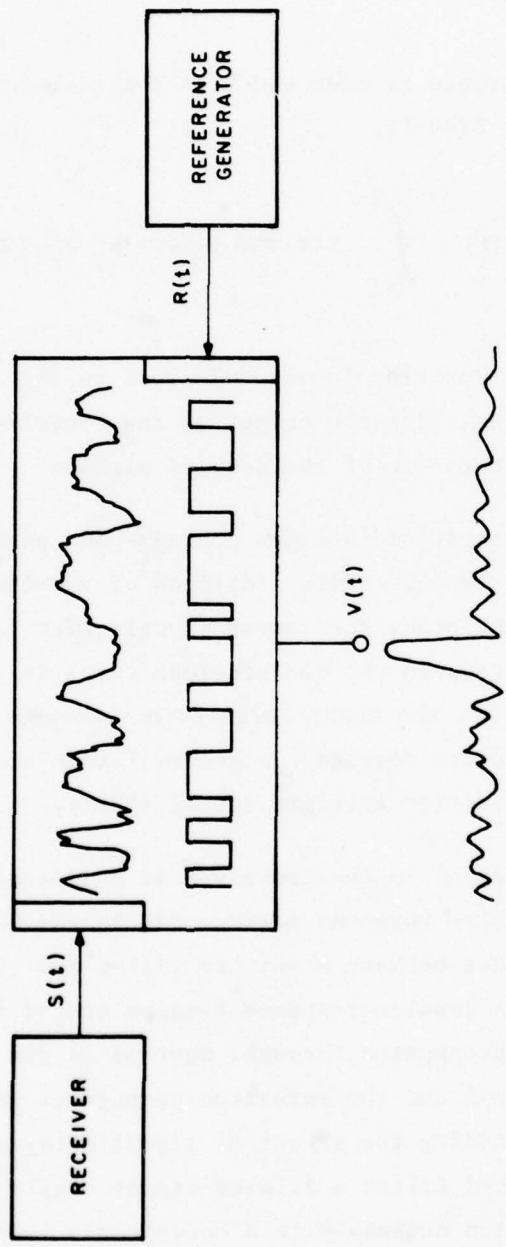


Figure 4.3 SAW Convolver

where T is the time interval corresponding to the interactive regions.

If the reference is made equal to the time-reverse of the signal, viz. $R(t) = S(-t-T)$,

$$V(t) = \int_0^T S(t-\tau) S(-t-\tau) = \phi_{SS}(2t),$$

where the signal duration is assumed equal to the time length of the interactive region. Thus the output of the convolver is the autocorrelation function ϕ_{SS} of the desired signal.

The autocorrelation function of wide-band pseudo-noise (PN) signals is a narrow pulse with sidelobes of varying amplitude on either side of the peak. For random signals with large time-bandwidth (TW) products the rms sidelobe level is $1/\sqrt{TW}$ times the peak (5). Similarly, the cross-correlation between two random signals is $1/\sqrt{TW}$ on the average. This correlation property is the basis for code-division multiple access (CDMA).

Behavior similar to the convolver is evidenced by a matched filter whose impulse response corresponds to the desired waveform. The main difference between a matched filter and the convolver is that the filter's impulse response remains stored in it while the received signal propagates through, whereas in the convolver both the received signal and the reference propagate. This difference has implications regarding the effect of signal delay or synchronization error. In a matched filter a delayed signal simply produces a delayed correlation output. With a convolver a loss of synchronism between reference and received signal causes a delayed output, but

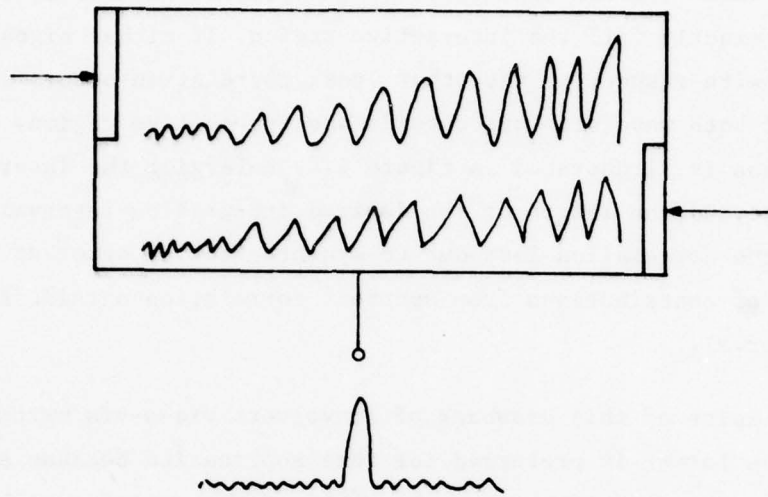
also a reduction in correlation amplitude. Maximum correlation results when waveform coincidence occurs at the instant that both signals exactly fill the interactive region. If either signal is delayed with respect to the other, peak correlation occurs when parts of both waveforms are outside the interactive region. This phenomenon is illustrated in figure 4.4. Enlarging the interactive region beyond the length of the desired integration interval will reduce the correlation loss due to synchronization error at the expense of contributions from spurious correlation outside the signal interval.

In spite of this drawback of convolvers vis-a-vis matched filters, the former is preferred for this application because significantly larger bandwidths are achievable. SAW convolvers at bandwidths of 100 MHz and TW products of 1000 have been demonstrated (6). Comparable TW products using matched filters implemented with charge coupled devices (CCD) are limited to bandwidths on the order of 10 MHz. Programmable SAW matched filters operate at TW products of 128.

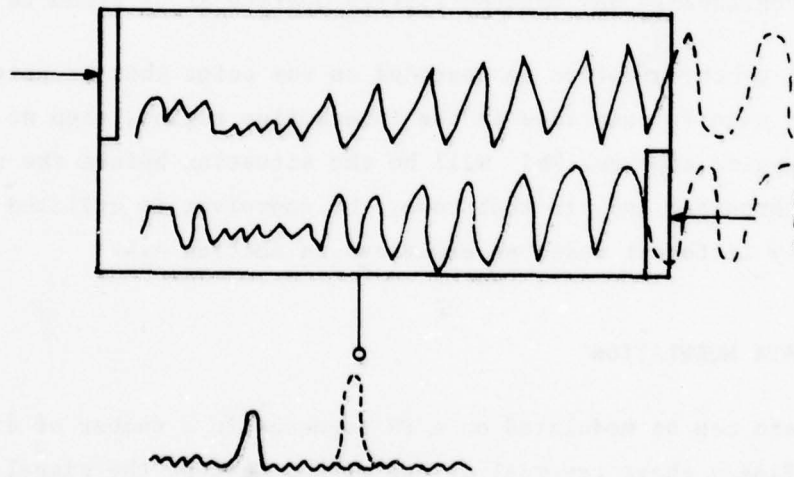
If synchronization is degraded to the point that no portion of the two signals coincides in the interactive region, then no correlation pulse appears. This will be the situation before the receiver is synchronized and, in that case, the convolver is utilized in a slightly different mode, as explained in section 4.4.

4.3 DATA MODULATION

Data can be modulated on a PN sequence in a number of different ways. Binary phase reversal is one method whereby the signal $S(t)$, consisting of a sequence of chips that represent one bit, is transmitted as $S(t)$ or $-S(t)$. Since the convolver's reference is



a) SYNCHRONIZED



b) UNSYNCHRONIZED

Figure 4.4 Effect of Delay Error

EA-51,339

positive, the correlation output is $\pm \phi_{SS}(2t)$. A coherent phase reference for detecting absolute phase is difficult to maintain, hence many systems employ differential phase-shift keying (DPSK). Information is conveyed by the phase-transition between successive bits, i.e., each bit interval serves as a phase reference for the succeeding interval. The DPSK approach using SAW convolvers has been implemented under the DARPA packet radio project (6) and could also be applied here. However, our objectives for data rate and TW product motivate the use of higher order signal alphabets: specifically a quaternary symbol alphabet is suggested. Complexity of the convolver system stands in the way of larger alphabets.

In each symbol interval one of four PN sequences is transmitted. At the receiver four convolvers are operated in parallel and a decision is made selecting the one with the highest correlation. Four sequences that are mutually orthogonal can be derived from a single PN code by simply multiplying the code by the four waveforms shown in figure 4.5 over each bit interval.

The probability of error in detecting multiple orthogonal signals in noise has been analyzed in the literature (7). A four symbol alphabet provides about 2 dB improvement over binary signaling.

It might be argued that the desired data rate could be achieved with less complexity by shortening the bit interval, i.e., reducing the effective convolver integration time. That approach would increase the CDMA cross-correlation (TW^{-1}) by 3 dB, but more significantly the potential for intersymbol interference due to multipath would be increased. Multipath produces multiple delayed pulses at the convolver output. If the delay spread is larger than the symbol duration, correlation pulses from successive symbols would be interleaved. On the other hand, if the delay spread is less than the symbol interval, the last multipath component from one symbol will

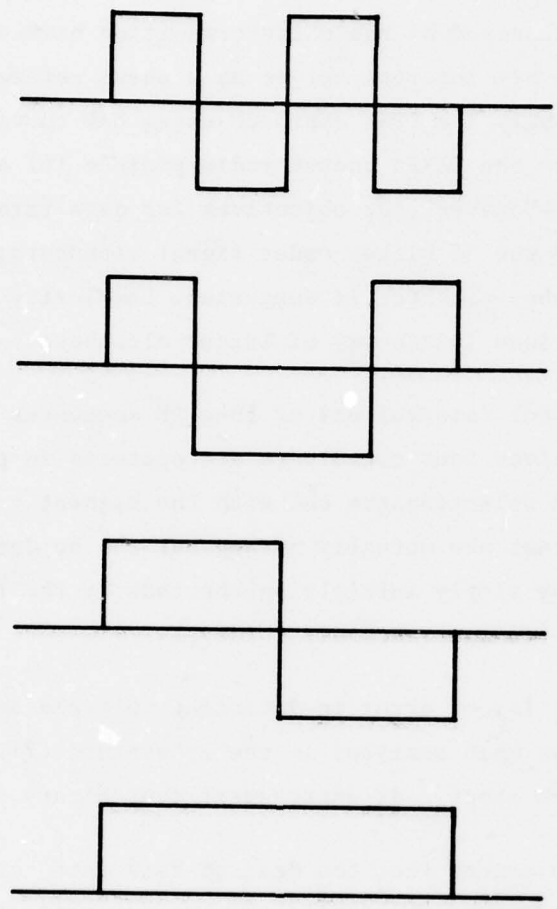


Figure 4.5 Four Orthogonal Waveforms

appear before the first component of the next symbol. Under those conditions there is intersymbol interference from correlation sidelobes only, and it is even possible to combine the signal energy from several resolvable delayed paths. Such combining provides a form of time diversity which is beneficial in communication over fading media. Moreover, the intersymbol interference due to sidelobes is reduced with the larger TW product. Thus, there is strong motivation to maximize TW and to gain data rate by higher order symbol alphabets.

4.4 SYNCHRONIZATION

A/J communications systems that utilize pseudo-random sequence generators to avoid predictability of the radiated waveforms, require synchronization between the generators at the two ends of the link. Convolver or programmable matched filters facilitate rapid synchronization; they do not require the lengthy search procedures of multiply-and-integrate correlators.

The synchronization process begins with a knowledge of the maximum time uncertainty of the receiver's clock relative to the expected signals. From this knowledge, including propagation delay uncertainty, the receiver can select, corresponding to the earliest possible arrival, a segment of the long pseudo-random sequence which is known, with high confidence, not to have arrived yet. This segment is one of a predetermined set, appearing periodically in the long sequence, that are used to establish synchronization prior to a message transfer. The segment corresponds to one integration interval of the convolver and is cycled repeatedly through the reference port. When the segment in question appears at the received signal port, a correlation pulse will appear during the next cycle of the reference. It can be shown, no matter what the timing of the

received signal relative to the repeated reference, that the correlation amplitude is no less than 0.75 of the maximum for perfect alignment of reference and received signal in the convolver interactive region. The arrival time of the correlation pulse relative to the start of the reference allows the local sequence generator to be synchronized to the received signal. Thereupon, the selected segment is no longer recirculated but the succeeding portions of the PN sequence are applied to the reference port. Two or more additional integration intervals should be used to confirm the first detection. After that, data modulation can start, and the receiver must decide which of four sequences was transmitted as described in section 4.4.

It may happen that no calls are attempted in a particular time span. Obviously, the receiver should not recirculate the selected segment indefinitely, because the counterpart of the earliest possible arrival is the latest possible arrival. When the time to the latter has elapsed, a new synchronization segment is selected to be cycled through the convolver. The new start-of-sync segment is far enough ahead in the PN sequence to assure that it has not arrived yet from the earliest possible source. This sequential step-search continues until a detection is made.

Similarly the sender may have to repeat the call attempt if the first try was unsuccessful, i.e., no response was obtained. After transmitting the synchronizing symbols, the sender listens for a reply starting with a predetermined segment. The sync acquisition procedure is the same as outlined above. If no reply is received after a suitable timeout, depending on propagation and clock uncertainties, the sender transmits again, beginning at a subsequent start-of-sync time. By the time the starting segment of this synchronizing sequence reaches the receiver, it also should have shifted to the appropriate segment.

Table 4.1
MODULATION PARAMETERS

CHIP RATE	200 MHz
SYMBOL DURATION	5 μ sec
TIME-BANDWIDTH PRODUCT	1000 (30 dB)
BITS PER SYMBOL	2
PEAK CHANNEL RATE	400 kb/s
HALF-DUPLEX NODAL THROUGHPUT	200 kb/s
LESS 50% OVERHEAD	100 kb/s

The separation between successive starts-of-sync should be longer than the time for which any receiver listens with a given PN code segment. If starts-of-sync occurred more frequently, then the undesirable situation would arise where some receivers are deaf to some starts-of-sync. Thus, the interval for start-of-sync is determined by the maximum anticipated time uncertainty among the nodes that are in communication range. The timing error is probably small for participating members of the net that have previously been synchronized. For new net entries this may not be true. Since the delay until channel access by net members is dependent on the frequency of occurrence of starts-of-sync, it would not be desirable to penalize them for time uncertainty of new entries. Therefore, different procedures are defined for new entries, as discussed in section 4.7.

4.5 MODULATION PARAMETERS

The preceding sections have described various aspects of the communications system including, in some instances, specific design parameters. The purpose of this section is to bring together the key parameters relating to the modulation scheme and data rate. Table 4.1 summarizes the parameters.

The occupied bandwidth of the PN signals is determined by the chip rate. A rate of 200 Mch/s has been selected based on a moderate projection beyond the current achievement of a 100 Mch/s convolver reported by MIT Lincoln Laboratory (6). The corresponding bandwidth of 300-400 MHz is reasonable from the point of view of percent of RF carrier (7 GHz) and possible allocation.

The selected symbol duration is $5\mu\text{sec}$, which is adequate to avoid serious intersymbol interference due to multipath for most types of terrain. Recall that as long as the delay spread is less

than the symbol duration, the correlation peaks from successive symbols are not interleaved. In that case intersymbol interference results only from correlation sidelobes which are on the order of $1/\sqrt{TW}$ relative to the peak. Consequently large TW products are beneficial to reduce multipath effects.

The duration of 5 μ sec is equivalent to 1000 chips/symbol. This number cannot be equated to processing gain because one symbol represents more than one bit. Two bits per symbol yields a raw data rate of 400 kb/s, and the processing gain expressed in terms of E_b/N_0 (energy per bit noise power spectral density) is 27 dB rather than 30 dB. This definition of processing gain ignores the fact that higher order alphabet transmission requires less E_b/N_0 than binary for the same performance. Nevertheless, the smaller value is used in the power budgets, and the E_b/N_0 requirements can be specified separately.

The half duplex operation (alternate transmit/receive) yields a throughput per node of 200 kb/s. Additional allowances must be made for inefficiency in channel utilization, e.g., synchronization procedures, routing data, acknowledgments. Assuming 50% effective utilization, the throughput per node is 100 kb/s.*

4.6 NODE CONFIGURATION

In this preliminary investigation design details were carried only to the level of the overall block diagram shown in figure 4.6. The antenna concept discussed in section 3.2 makes available a number (e.g., 12) of simultaneous receive beams and only one of a

*The nominal rate does not include redundancy for error control. Overhead for error control should be included in the traffic requirements.

IA-51,739

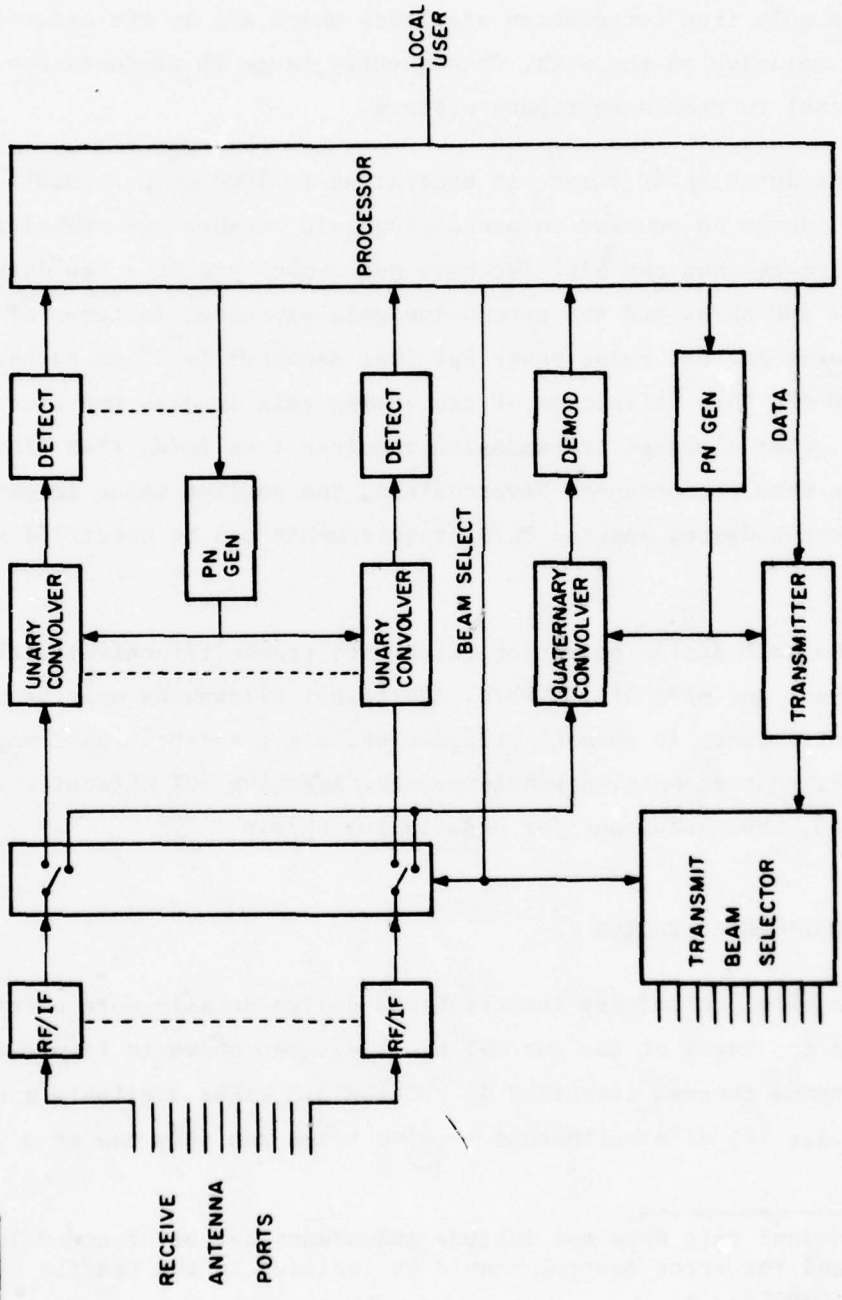


Figure 4.6 Node Block Diagram

larger number (e.g., 72) of transmit beams. Multiple receivers (amplification and RF to IF conversion) monitor the beams and provide inputs to a set of unary convolvers. A unary convolver is used to detect the presence or absence of a selected PN segment.* In contrast, the quaternary convolver is in effect four convolvers in parallel, allowing a decision (demodulation) selecting one of four possibilities. One receiver is switched to the quaternary convolver while traffic is being carried on the respective beam. The other receivers are connected to the unary convolver to await synchronization signals or acknowledgments to specific transmitted packets.

The remainder of the block diagram shows the interconnection of the nodal processor and the other elements of the system. The functions represented by these blocks are believed to be self-explanatory.

4.7 NET ENTRY

The requirement of mobility for C³ facilities has a corollary need for prompt operational status after redeployment. For the communication support system this implies automatic connectivity procedures between a new entry and the existing network. The azimuthal direction of neighboring nodes must be found to permit accurate aiming of directional antennas and time synchronism must be established to within the uncertainty tolerance of the net participants.

Passive and active net entry procedures have been considered. In the passive mode a new entrant remains in a listening status until an established member transmits in its direction. This mode

*The choice of unary is dictated by cost considerations. If the cost differential is sufficiently small, quaternary convolvers would be used on all receivers.

has the advantage of minimizing the new entrant's exposure to enemy intercept before the node is involved in message traffic. A disadvantage is that some or all established nodes must conduct a search for new entrants. The active procedure places the burden of initiating transmissions on the new entrant. Details of the latter approach are explained in the following paragraphs.

Under some circumstances the net entrant may have prior knowledge of the relative location of neighboring nodes and can, therefore, immediately aim its beams in the desired direction. However, if the relative position data is unavailable or inaccurate, the new entrant must execute an azimuth as well as a time synchronization search. Depending on the extent of prior uncertainty the azimuth search may cover limited sectors or a full circle.

Azimuth search can be accomplished by sequentially stepping the transmit beam and emitting interrogations at each beam position. Network nodes within communications range will detect the interrogation transmitted on the common PN code. Direction of arrival will be determined only with the relatively broad beams of the multiple receiver configuration. The reply will be transmitted rapidly in succession over the several adjacent narrow beams overlapping the coverage of the beam that received the interrogation. This procedure allows the entering node to use its lower gain receive beams to listen for replies. Alternatively, the reply can be sent on the broad beam while the entering node's receiver is connected to the high gain antenna, thereby maintaining the gain product constant in both directions on the link. It is probably desirable for antenna simplicity to avoid transmitting and receiving on both the broad and narrow beams. For that reason the succession of narrow-beam transmitted replies will be assumed for this discussion. When a reply is

received by the interrogator the azimuth of the respondent node is recorded for future exchanges.

The interrogation and reply are both short sequences of symbols that convey no data, but are used merely to determine azimuth directivity for the entering node. After the entering node has stopped its search, the previously established node performs a small sector search to find the azimuth of the new node.

Because of time uncertainties, it may be necessary to transmit a series of interrogations with different time offsets of the local clock. One of the trial time offsets would generate a PN code sequence that falls within the delay acceptance limits of nodes in the established network. (See section 4.4.)

It is of interest to calculate the time to complete a search for a representative situation. Assume that the timing uncertainty for the new entrant is a factor of 1000 larger than the net participants, e.g., 200 μ sec net uncertainty including differential propagation delay among directly communicating nodes and 0.2 sec clock uncertainty for a new entrant. Hence, 1000 trials are required for time synchronization.

An interrogation may consist of 5 symbols (25 μ sec) and the succession of replies a total of 30 symbols, assuming that transmit beams are 1/6 the width of receive beams. The 35 symbols occupy a total time of $35 \times 5 = 175 \mu$ sec. The round trip delay for a reply, including propagation and processing delay, could range from 100 μ sec to 300 μ sec. For the straightforward approach of transmitting and waiting at each azimuth, the time per beam dwell would be a maximum of $1000 \text{ trials} \times 475 \mu\text{sec/trial} = .475 \text{ sec/beam}$.

A more efficient approach takes advantage of the relatively broad receive antenna beams and multiple receivers. In this case interrogations would be emitted into several narrow beams in succession during the time interval before the earliest arrival in reply to the first interrogation. For the above parameters four interrogations could be sent before the earliest reply. These interrogations would all pertain to the same trial time sync. The time per four trials is now the sum of the minimum delay and the maximum delay plus the interrogation and reply time. The time per beam for 1000 trials is then $1000 \times 1/4 (100 + 475) = .144 \text{ sec/beam}$ roughly one-third the previous result.

A search covering 360° with 72 beams would consume 34.2 sec in the former case and 10.4 sec for the latter, more efficient approach. Neither search time poses any serious problem for operations where new net entrants arrive infrequently.

SECTION 5

MESSAGE ROUTING

Every message has an origin and a destination; the destination can be a single address, multiple addresses, or everyone in the system. The messages destined for single or multiple addressees are termed directed or point-to-point messages, and those intended for all nodes in the network fall under the heading of broadcast messages. The term "broadcast" is used even though multiple relayed transmissions are generally required to convey a message to all possible destinations. Because the origin frequently cannot communicate directly with the destination, routing protocols are necessary to forward messages via several intermediate nodes.

This section discusses in some detail a particular candidate routing procedure, viz, local adaptation of routing tables based on message traffic. Global preprogrammed algorithms based on a knowledge of total network connectivity are also mentioned briefly.

5.1 DIRECTED MESSAGES

5.1.1 Routing Tables

The routing tables stored at each node define the path that a message follows as it propagates through the network. A routing table for directed traffic has an entry for the destinations that are accessible from the node by some path through the network. For every such destination there is a list of one or more nodes termed "successors", i.e., those nodes that are within radio propagation

range and are potential next hops en route to the destinations. Associated with each destination/successor pair are parameters related to the goodness or quality of the route in question. Possible parameters of the route are the number of relay hops to the destination and the minimum signal margin (measured with respect to noise or jamming) for the weakest link on the route.

In using the routing tables the node processor looks at the destination on the header of a message to be forwarded, enters the table, and selects a successor according to a specified criterion.

Several methods exist for creating and updating the routing tables. The two main categories are local adaptation and global procedures as described in more detail below.

5.1.2 Local Adaptation

This category of routing table adaptation is distinguished by the fact that the information for creating and updating routing tables is derived from the headers of messages in transit or by exchanging data among adjacent nodes. Knowledge of the connectivity of all network participants is not necessary. Local adaptation, or what is sometimes called distributed routing algorithms have been investigated by several researchers. The candidate approach described below was evolved by Sussman and Witt and is based in part on the work of Baran (8) and Boehm (9), who introduced the concept of "backward learning" for routing table updating, by observing that messages passing through a node from a specific origin imply the existence of a path from that node backwards to the origin. The prior node on the message path, denoted the "predecessor," corresponds to the successor in the routing table, and the message origin corresponds to the destination entry in the table.

This concept is predicated on reciprocity, i.e., all nodes are bidirectionally connected if at all.

If the message header carries a measure of route quality, such as the number of hops traversed, and if messages are forced to take alternate paths by some mechanism, then the routing table can be updated to converge to the best path. Improved routes can be discovered and recorded by assuring that a sufficient number of new paths are attempted from each origin. One simple procedure is to send flood-routed messages (see section 5.2) that pass over all links, thereby allowing comparison among all possible paths. Unless done infrequently, flood routing increases the message traffic and leads to inefficient operation. Another approach is to employ alternate paths when the primary (current best route) successor is busy. Random routing to discover new and possibly better paths is still another method of updating the routing tables.

The converse process of either deleting paths from the routing tables or modifying the path quality downward when changing conditions indicate is an essential ingredient of adaptive operation. Periodic flood-routed messages from every origin to every destination permit total purging and renewal of all routing tables. But, again, this straightforward approach consumes more network capacity than may be necessary. Another procedure for identifying network degradation and modifying routing tables accordingly takes place as follows: A subset of messages, e.g., priority traffic, will attempt to follow the currently established best path as defined by the routing tables. However, if the best path reveals a break because of node or link disruption, the best-path message will be routed onto the highest ranking alternate path. At each node along the route, the path parameters in the message header are compared to the entries in the routing table to determine the primary path

to the message origin. If the best-path-routed message is on a route that is different or inferior to the current primary route, the current routing table entry is replaced by the information derived from the message header.

Note the the replacement of best path in the routing table by a poorer path does not occur when a message takes an alternate route to avoid a temporarily busy node. In that case, the routing table is updated only if the alternate path is better than the former.

5.1.3 Prior Message List

To facilitate the local adaptation process, a list of recently handled messages is stored at each relay node. The list serves two purposes: it detects the existence of looping messages and it provides information for retracing the same route in the forward or reverse direction. The list contains the information in the message header, the node it came from (predecessor), and where it went (successor).

Since a closed loop path can arise as a result of alternate route selection, each message carries a unique identification to enable reappearance of the same message at a node to be detected. When a received message identity matches one stored in the prior message list, an alternate successor is selected, and the new successor is written in place of the old one. The stored predecessor addresses are needed to reconstruct the message route in the reverse direction for end-to-end acknowledgment.

5.1.4 End-to-End Acknowledgment (ETE-ACK)

The ETE-ACK confirms reception of individual messages at their intended destinations. In addition, the ETE-ACK provides a mechanism for updating routing tables with entries for the destination of the original message. The ETE-ACK follows the original message route in the reverse direction using the predecessor information stored in the prior message list. Loops are not retraced. The information in the ETE-ACK header is used to update the tables with loop-free paths in accordance with the rules applicable to the class of message being acknowledged -- best-path-routed or not. This procedure causes the successful forward route to be recorded in the routing tables as necessary.

5.1.5 Flowchart

The key features of the local adaptation algorithm described earlier are embodied in the flowchart of figure 5.1. The chart defines the processing for relayed messages and the routing table modification procedures. Other important elements, including hop-by-hop acknowledgment and final destination processing, are not illustrated.

A computer simulation of the local adaptation procedures is being developed to test the performance of the concept for its response to network changes as measured by message delay.

5.2 FLOOD ROUTING

The term flood routing or saturation routing is applied when messages are transmitted on every available link regardless of destination. For point-to-point messages, flood routing is generally

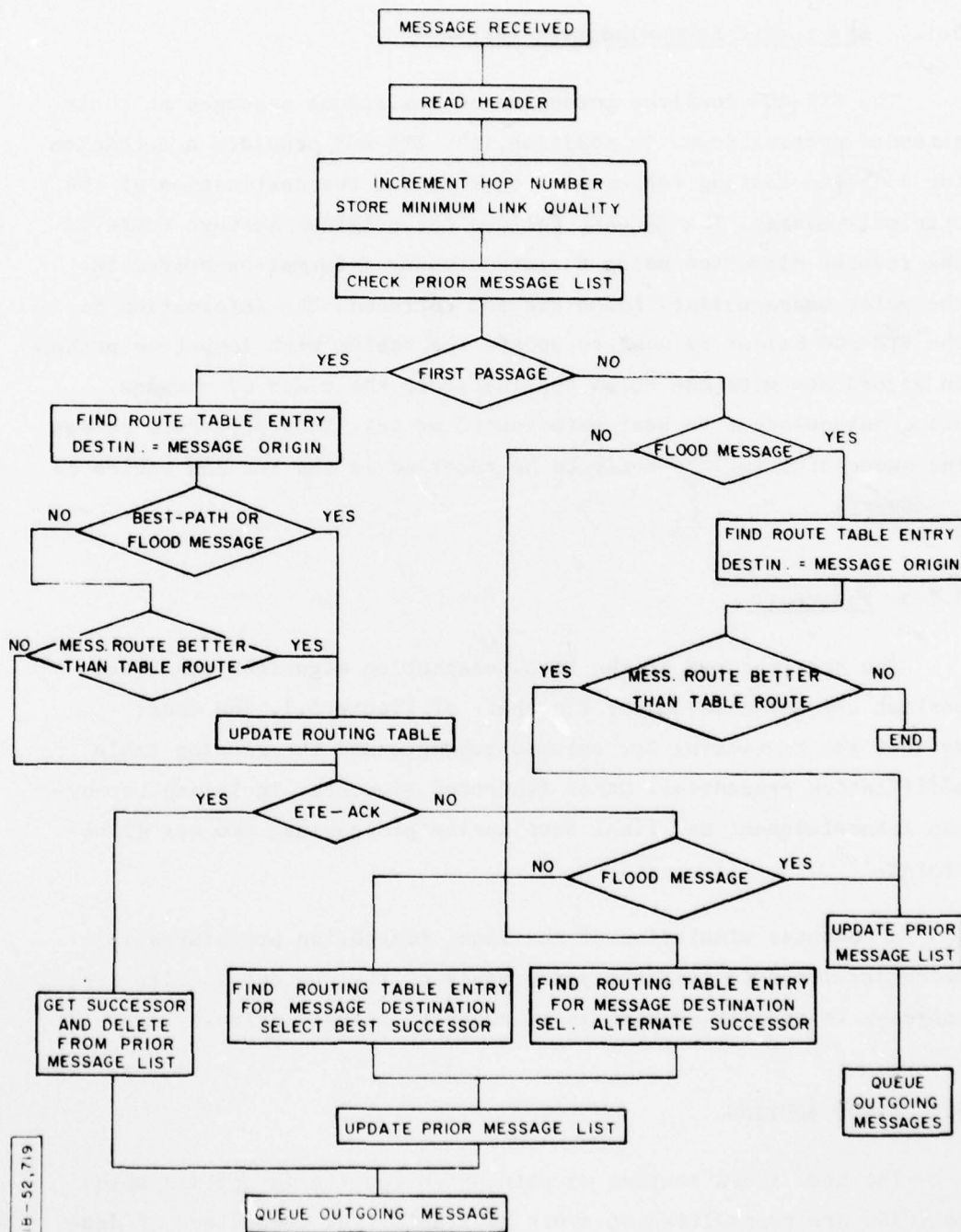


Figure 5.1 Flowchart for Adaptive Routing Strategy

avoided except as a search method to find subscribers whose location is not known (9). For broadcast messages, flood routing has the advantage of placing a small processing burden on each node only to prevent message looping (see section 5.1.3). Broadcasts can proceed without knowledge of global connectivity and without consulting routing tables. Such simplicity is purchased at the price of redundant transmissions reflected in greater traffic capacity requirements.

5.3 GLOBAL PROGRAMMED ALGORITHMS

A number of algorithms exist for deriving the network routing tables, given the knowledge of network connectivity and a criterion of path quality based on number of hops or other measure associated with each link on a route. The algorithms can be executed by a central facility and the routing tables distributed to each node, or the connectivity information can be disseminated for each node to compute its own routing tables. Well-established responses to network disruption and adaptive procedures for the global algorithms are lacking, however, making this approach appear less attractive for a survivable network. However, ongoing research in this active field may produce adaptive routing strategies to meet the desired objective.

SECTION 6

FUTURE WORK

As indicated throughout, a first-cut possible design concept for a future survivable communications network has been presented here. The report is intended to stimulate further activity on this subject. All the issues need to be explored in greater detail, tradeoffs evaluated and alternatives considered. Specific topics that need attention are:

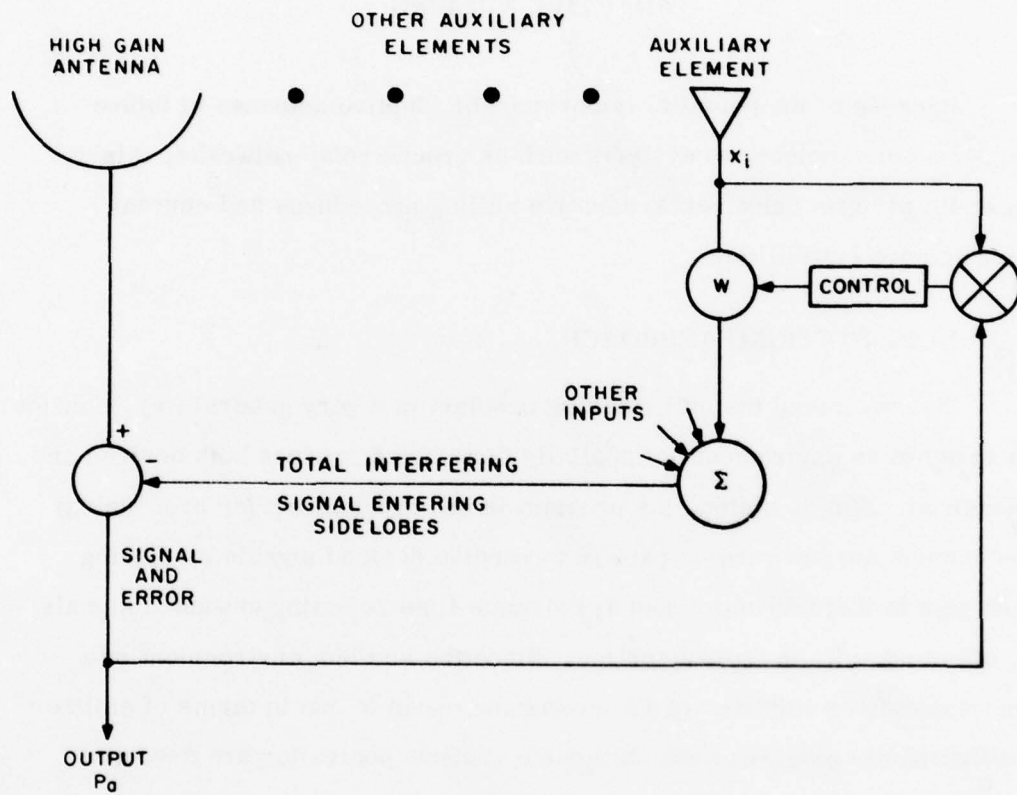
1. A reexamination of the RF design (antennas, modulation, and so on) to support net entry, link establishment, and message transfer.
2. The design impact of incorporating airborne nodes.
3. Evaluation of data capacity and message delay performance.

APPENDIX A
ADAPTIVE NULLING

Because of the potential importance of adaptive antennas in future anti-jam communications systems such as ground relay networks, this appendix reviews fundamental adaptive nulling procedures and current performance capabilities.

A.1 NULL STEERING APPROACH

To understand the null steering problem in a very general way, consider an array in an environment of spatially distributed sources both desired and undesired. Simply stated, the problem is one of adjusting (or processing) the antenna system receive pattern to receive desired signals by placing high gain in their direction and at the same time rejecting unwanted signals by effecting nulls in their direction. Since the ambient environment of a communications receiver is a complex and dynamic one in terms of emitter configuration, adaptive methods for the process controller are essential. Early studies into interference nulling led to a scheme for an auxiliary antenna to sample an interferer and subtract its received signal from the main channel by proper adjustment of amplitude and phase. This so-called sidelobe canceller is shown in figure A.1, where only one channel of processing is included. The total signal X_i in the i^{th} channel is made up of a desired signal, an interferer, and the various environmental and circuit component generated noise elements. These signals are complex weighted and summed to form the system output P_a . It is assumed that one channel is a highly



IA-51,348

Figure A.1 Sidelobe Canceller

directive antenna pointed at the desired signal and that the level of this signal is considerably lower than the interferer. The output signal or some error signal is correlated with the signal X_i in each channel and after suitable filtering provides the control voltage for the channel weighter. The correlator output voltage drives the channel weight until minimum correlation exists corresponding to minimum jamming power in the output.

In the more general adaptive array configuration no high gain antenna is utilized and all elements of the array are the same. If an error signal is formed by removing the desired signal from the total output, the error is minimized by minimizing jamming and noise only. Since the desired signal components in each channel will not correlate with the error, they will not be reduced. If on the other hand, the signal cannot be recognized and removed it will be suppressed along with the interference and thermal noise. When substantial correlation exists between X_i and the error signal, the correlation will modify the weight. This procedure will continue until minimum correlation exists and the error signal is minimized.

The difference between the various adaptive techniques is in the a priori information used, the measure of performance, and the manner in which the complex weight settings are evaluated and incremented.

A.2 PERFORMANCE MEASURES AND OPTIMIZATION TECHNIQUES

A number of solutions have been suggested for deriving the optimal weight vector. However, before we can define an optimal solution, a performance criterion for the array output must be established. Several such criteria have been suggested, the most important among them being mean square error, signal-to-noise ratio, and total power. These criteria form the basis for two of the most commonly used algorithms: Least Mean Square

(LMS), after Widrow (10), and Maximum Signal-to-Noise (MSN), after Applebaum (11).

Given these measures, various techniques are available for their optimization. In general, these approaches can be placed into two categories: search and gradient, or first-order, methods.

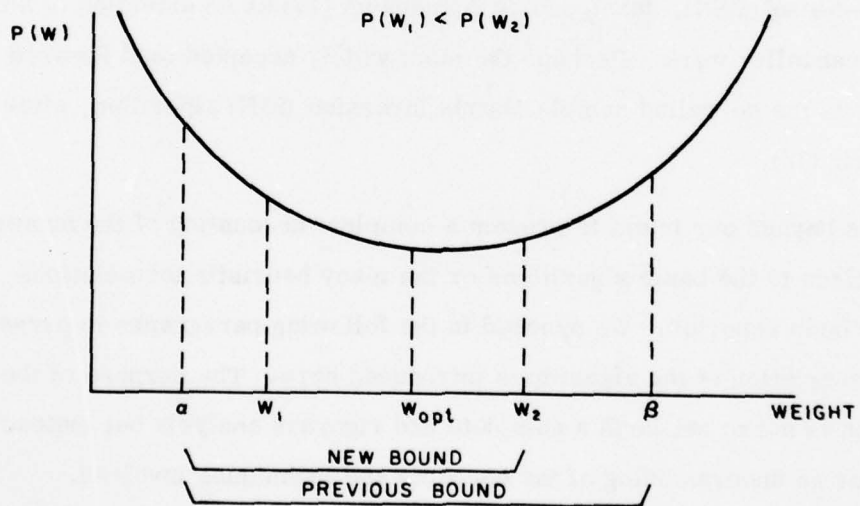
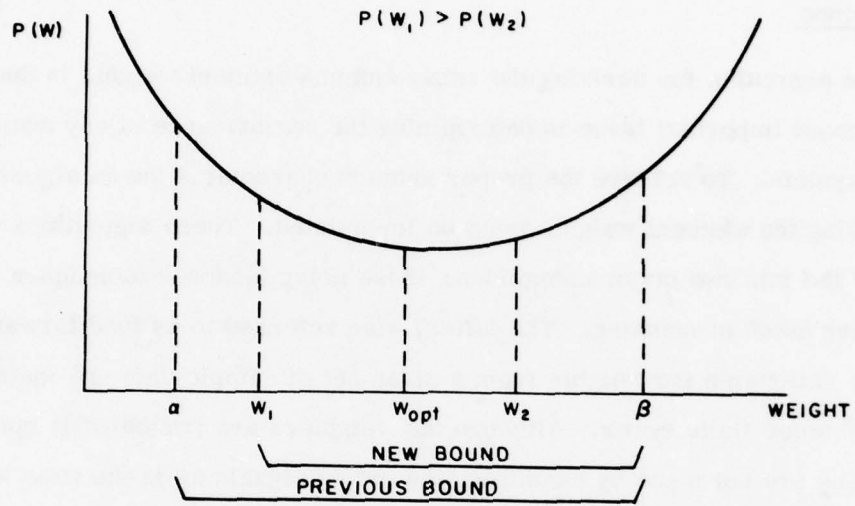
The search methods are essentially sophisticated trial-and-error schemes. They proceed by evaluating the performance measure for several values of the weight and from these calculations make an improved weight estimate. By way of illustration, consider the two situations shown in figure A.2 for the initial weight approximation W_1 . If the optimum weight (W_{opt}) can be bounded by $[\alpha, \beta]$, a smaller boundary region can be established as follows. Let $\alpha < W_1 < W_2 < \beta$ and the performance measure be represented by $P(W_x)$. Then for:

case (1) $P(W_1) > P(W_2)$ W_{opt} is bounded by $[W_1, \beta]$

case (2) $P(W_1) < P(W_2)$ W_{opt} is bounded by $[\alpha, W_2]$

The next trial is compared to $P(W_2)$ for case (1) and to $P(W_1)$ for case (2); the process continues until the corrections are small. Various methods are available for choosing the next trial and it is this method that defines the specific algorithm.

Gradient or first-order techniques use knowledge of the gradient of the performance measure for a candidate weight setting to generate an improved weight estimate.



IA-51,547

Figure A.2 Search Method

A.3 ADAPTIVE ALGORITHMS

A.3.1 Scope

The algorithm for deriving the array antenna element weights is doubtless the most important issue in determining the performance of any adaptive antenna system. To achieve the proper antenna characteristics an algorithm for choosing the element weights must be formulated. These algorithms can be separated into two major categories: those using feedback techniques and those using batch processing. The latter, also referred to as feed forward systems, determine the weights from a given set of sample data and install them with some finite error. Although the weighters are periodically updated, corrections are not made by examining the output signals as is the case in feedback systems. The most widely accepted and effective feedback algorithms are the Least Mean Square (LMS), attributed to Widrow (10), and the Maximum Signal-to-Noise (MSN), developed by Applebaum (11) as an extension of his sidelobe canceller work. Perhaps the most widely accepted feed forward technique is the so-called Sample Matrix Inversion (SMI) algorithm, after Reed et al. (12).

It is beyond our intent to present a complete accounting of the numerous modifications to the basic algorithms or the many heuristic formulations that have been reported. We proceed in the following paragraphs to present a brief description of the algorithms introduced here. The purpose of the discussion is not to set forth a complete and rigorous analysis but instead to transfer an understanding of the concepts and techniques involved.

A.3.2 Maximum Signal-to-Noise Algorithm

The technique is basically one to maximize the signal-to-noise in any noise environment by considering minimum output noise as the measure of

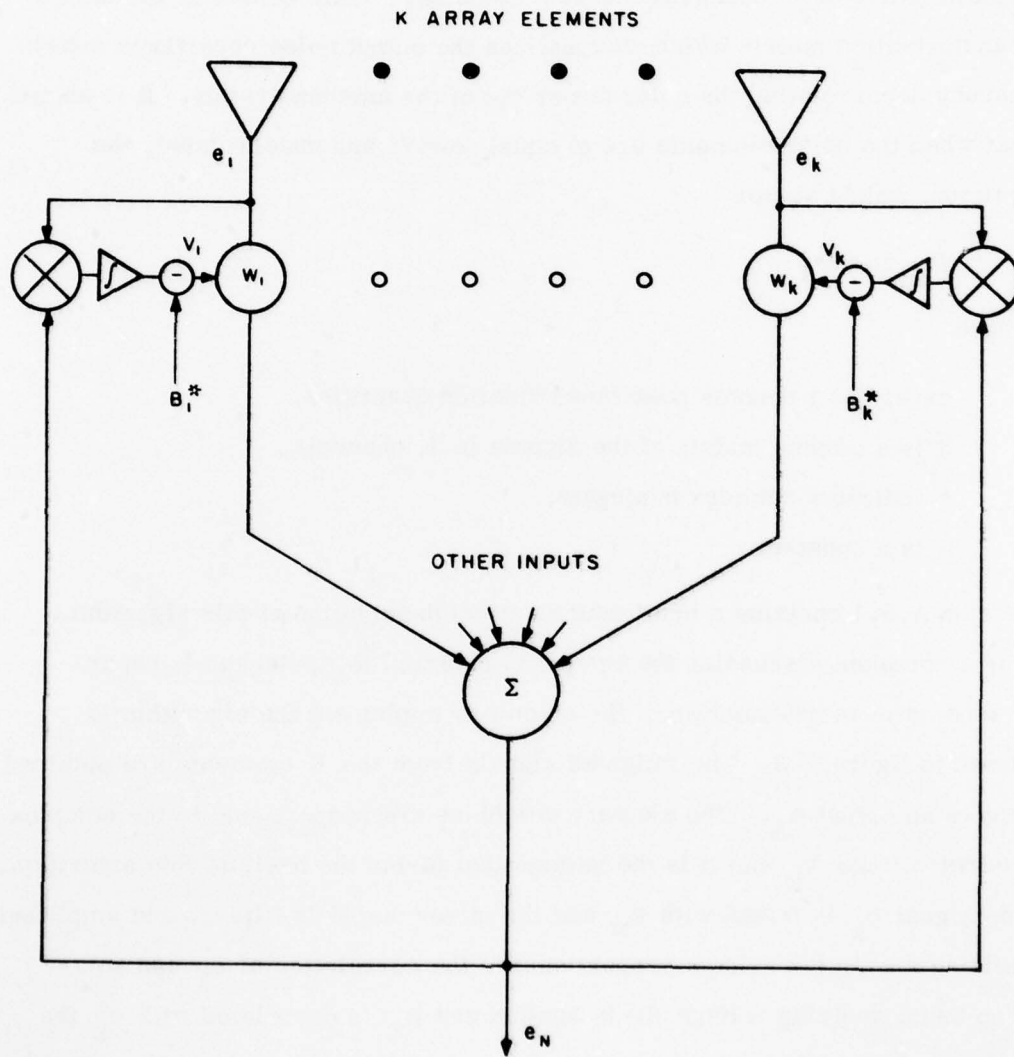
performance. The algorithm has been described in mathematical terms by Applebaum (11). An expression is derived for the optimum weights through the utilization of an optimum coherent combiner. This combiner includes a transformation matrix which diagonalizes the output noise covariance matrix, thereby decorrelating the noise power out of the antenna system. It is shown that when the noise elements are of equal powers and uncorrelated, the optimum weight vector

$$\hat{W}_{\text{opt}} = \mu S^*,$$

where

- caret (^) denotes posttransformation quantities,
- S is a column matrix of the signals in K channels,
- * indicates complex conjugate,
- μ is a constant.

Section A.5.1 contains a brief mathematical description of this algorithm. For a complete discussion the reader is referred to Applebaum's paper. A schematic representation of the circuit to implement the algorithm is shown in figure A.3. The weighted signals from the K elements are summed to give an output e_N . The element weighters are proportional to the complex control voltage V_k and it is the voltage that forms the basis of this algorithm. The signal e_k is mixed with e_N and the mixer output is filtered and amplified yielding a complex voltage proportional to the correlation of e_k and e_N . If no beam steering voltage (B) is applied and e_N is correlated with e_k the low pass filter integrates the output of the correlator to produce V_k , changing the weight W_k to reduce the correlation between e_k and e_N , which further reduces the correlation output. A similar performance by the K loops reduces e_N to a minimum. In the absence of a beam steering voltage, any signal detected by the loop will be reduced to the noise level. If a desired



IA-51,546

Figure A.3 MSN Algorithm Representation

radiation direction is known, beam steering or constraining voltages (B^*) can be applied to the weighters to effect a directional collecting aperture. Consider that beam steering voltages (represented by matrix B^*) are used to steer the beam in the direction ϕ_o . In the quiescent case (no interferers) the element weights necessary to generate a pattern in the direction ϕ_o can be denoted by a vector W_{qt} . When noise interference exists in the loop, however, the weight W_k of the k^{th} element is equal to the beam steering voltage B^* minus the output V_k of the associated correlator such that

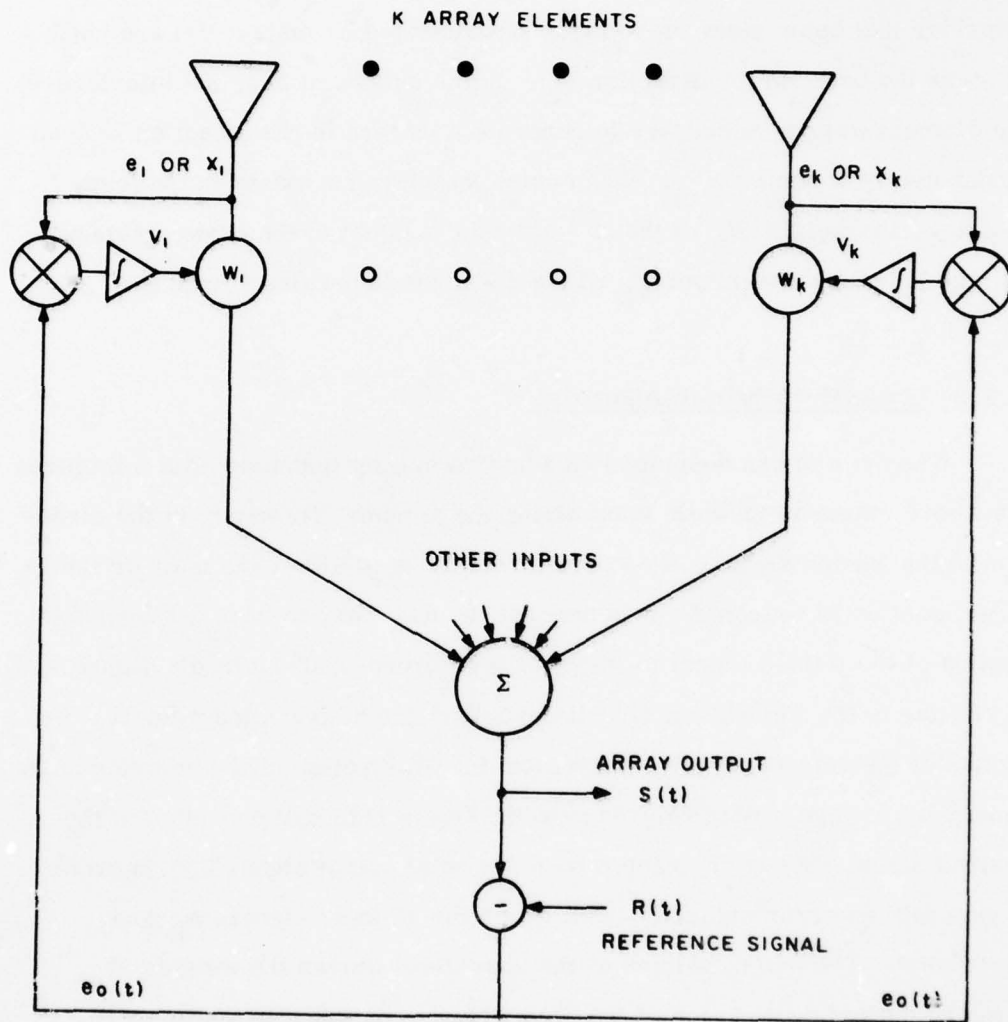
$$W_k = B^*_k - V_k.$$

A.3.3 Least-Mean-Square Algorithm

Widrow (10) has described an adaptive nulling technique that minimizes the interfering source while maximizing the antenna directivity in the direction of the wanted signal. No a priori knowledge of either the user or interferer location is required. It is necessary, however, to have a reasonable replica of the wanted signal to inject as a reference. The circuit (figure A.4) is similar to the Applebaum circuit described previously except for the injection of the reference at the output and the elimination of the steering beam constraint voltage. With reference to the figure note that a replica of the desired signal $R(t)$ is subtracted from the total output signal $S(t)$ in order to generate an error signal e_o with which the K input signals e_k are correlated. The output voltage of the correlator drives the weights W_k . A mathematical description of the algorithm is contained in section A.5.2.

A.3.4 Sample Matrix Inversion (SMI)

One practical optimum value of the element weighters is the weight, W_o , which maximizes the signal/noise ratio as discussed in section A.3.2.



IA-51,545

Figure A.4 LMS Algorithm Representation

AD-A064 440

MITRE CORP BEDFORD MASS

F/G 17/2.1

A SURVIVABLE NETWORK OF GROUND RELAYS FOR TACTICAL DATA COMMUNI--ETC(U)

DEC 78 S M SUSSMAN, L G DARIAN, K W RAU

F19628-78-C-0001

UNCLASSIFIED

MTR-3647

ESD-TR-78-181

NL

2 of 2
AD
A064440



END
DATE
FILMED
4-79
DDC



MICROCOPY RESOLUTION TEST CHART

This value was given by $W_o = \mu M^{-1} S$ and the optimal value of S/N is given by $(S/N)_o = S^* M^{-1} S$, where S is the complex signal component and M is the noise covariance matrix with M^{-1} its inverse. For instance, S could be DOA information used to steer the beam in some desired direction.

The W_o equation above cannot be implemented if neither S nor M are known a priori. The SMI algorithm reported by Reed (12) is basically a method for establishing M in the absence of desired signals* through an output signal sampling technique.

Reed obtains an estimate of M which he calls \hat{M} by applying the maximum likelihood principle of statistical estimation. It turns out that M is the arithmetic average of the sample noise matrixes $X^{(j)} X^{(j)*}$ for $j = 1, 2, \dots, K$ samples. \hat{M} is the sample covariance matrix.

\hat{M} is then inverted and the optimum weight becomes

$$\hat{W}_o = \mu \hat{M}^{-1} S.$$

In practice, inversion of M is lengthy and unwieldy, hence steps have been taken to shorten the process by selectively operating on \hat{M} (13).

A.4 FACTORS AFFECTING NULLING PERFORMANCE

A number of critical parameters affect the capability of an adaptive antenna to produce discriminating nulls in the radiation pattern. Most important among these are bandwidth, adaptation time, and number of jammers. A brief discussion of each of these parameters and some results reported by others are included. The results are not meant to indicate

*One scenario that might be envisioned is to steer the antenna to an omnidirection pattern [$S = (1, 0, 0 \dots 0)$] and sample M when no friendlies are radiating.

expected or typical behavior patterns since this obviously requires more in-depth analysis. Rather they are meant to put into perspective some of the more critical issues governing the nulling capability of an adaptive system.

A.4.1 Bandwidth

One of the major factors limiting jammer null depth is the bandwidth over which the array must operate. A typical array utilizing phase and amplitude control over the radiating elements is inherently a narrow-band device. A bandwidth increase results in increased array dispersion as well as dispersion in the circuit components. Dispersion causes the phase in adjacent channels to be a different function of frequency, effecting a non-linear phase/frequency curve in the sum channel. The main beam effect of increased bandwidth is well-known and certainly an important consideration in array antenna design. A null, however, is much more sensitive to frequency, and control of its depth and position puts great demands on the wideband performance of system components such as phase shifters, radiators, and so on.

Array Dispersion. The null degradation attributed to the geometry of the array and the distance between elements is caused by the requirement for a signal to traverse the elements that comprise the antenna aperture.* The phase weighting is correct only for signals arriving broadside to the aperture or at center frequency, and phase errors increase with frequency, bandwidth, and scan angle off boresight. The degradation can be analyzed from two viewpoints: null depth and null direction. The null depth is inversely related to the bandwidth and scan angle off boresight.

*Assuming fixed phase weighting.

Abrams (14) has derived an expression for the null depth for the two-element array case, which is given as

$$C = 10 \log \left[2 - \frac{2 \sin \left[\frac{\pi}{100} (B) \left(\frac{d}{\lambda} \right) \sin \phi \right]}{\frac{\pi}{100} (B) \left(\frac{d}{\lambda} \right) \sin \phi} \right],$$

where

- B = percentage RF bandwidth,
- d = wavelength spacing between elements,
- ϕ = scan angle off boresight.

Figure A.5 is a plot of the above expression for the half wavelength element spacing case. Note that the null depth varies inversely as the square of the bandwidth.

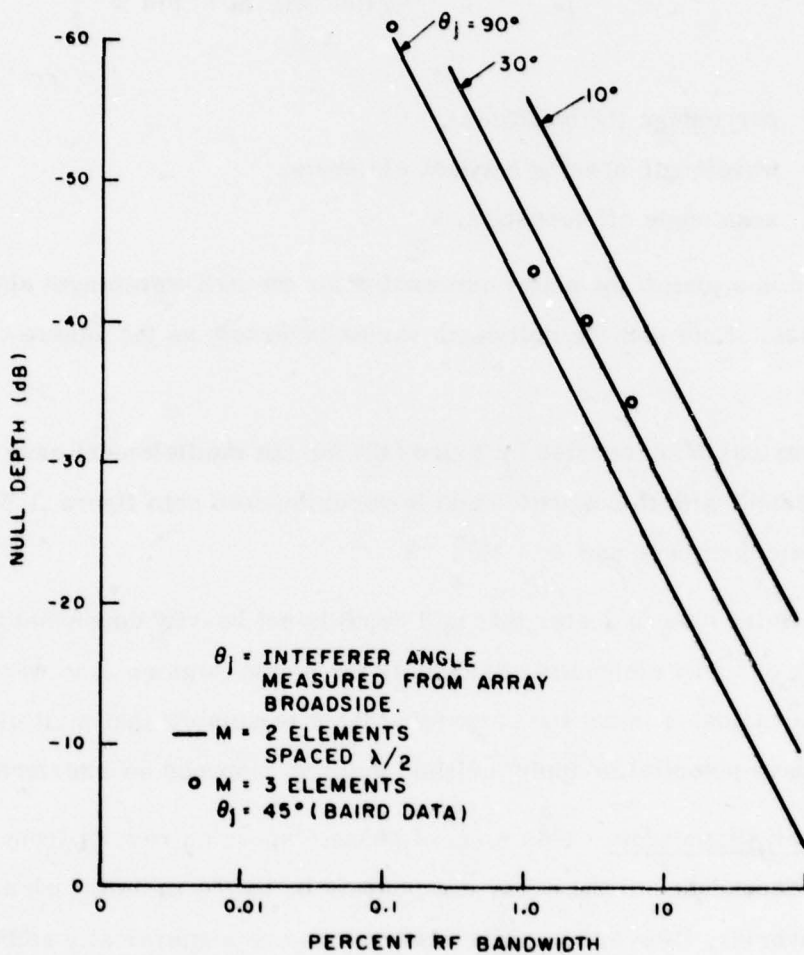
Numerical data reported by Baird (15) for the multielement case shows good agreement with this equation and is superimposed onto figure A.5 for the three-element case and $\theta_j = 45^\circ$.

The Baird data indicates that null depth is not heavily dependent upon the number of array elements. Since only the single jammer case was dealt with, this conclusion is not too surprising if we remember that multiple elements have potential to apply multiple nulls to suppress an interferer.

Circuit Dispersion. This form of phase dispersion results from the frequency dependence of the array components including radiating elements, weights, hybrids, filters, etc. The dispersions are algebraically additive and create an overall dispersive phase error at the array summing junction.

A.4.2 Adaptation Time

It can be shown (15) that for a single interfering source the loop time constant can be expressed as:



IA-31,344

Figure A.5 Array Dispersion

$$\tau = \frac{t_o}{KGP_{in}},$$

where

τ = loop time constant,

G = loop gain,

K = correlator conversion constant,

P_{in} = loop input power,

t_o = integrator (filter) time constant.

The loop gain should be set sufficiently high to minimize the adaptation time but not high enough to cause instability. To prevent instability the loop gain should be set in accordance with the strongest jamming signal expected. This will determine the weakest signal that can be handled in a given time. Hence the strongest jammer is initially reduced very rapidly to a level somewhat above steady state. It is then reduced at a slower rate until all interferers are reduced to a steady-state level. It is extremely important to adjust the loop gain so the weakest expected interfering signal will render a tolerable loop time constant. If there is an excessive spread in the signal strength of the jamming signals, it may be rather difficult if not impossible to choose a suitable gain value. It has been shown (16) that the convergence rate is also dependent upon the number and angular position of the interferers.

Present indications are that for analog implementations of the feedback approach, convergence times on the order of 20 μ sec are being measured for the single jammer case.

For digital control circuit implementation, the array convergence response is limited by the repetition rate of the computer or microprocessor used to perform the algorithm computation and element control functions. Figure A.6 is an example of the computed convergence response function obtained by performing a search algorithm to adapt a 21-element array (17). The null depth average over a 5% bandwidth on each of 3 jammers versus time (measured in computer iterations) is shown. Note that a null depth of more than 38 dB below peak is reported for each jammer after 70 iterations. The availability of initial beam weight knowledge is crucial to the null depth resulting from a few iterations and indeed to the total number required for convergence. According to the report none was utilized.

More current measured data being reported by Harris (18) indicates that maximum null depth is attained after approximately 100 iterations for the single jammer case. Although a quick comparison with the earlier report raises a few questions, more details of each experiment would be necessary to make a valid comparison. The important point here, however, is that 100 iterations seems a reasonable order-of-magnitude computing figure for the present. The absolute time for convergence (T) would of course be:

$$T(\text{sec}) = \frac{\text{No. computer iterations}}{\text{Computer repetition rate}}$$

with repetition rate in iterations/sec.

The tradeoffs involved in choosing the most effective computing device for any adaptive system are obviously many and complex and well beyond the scope of this report. As an illustration of some of the current technology, Harris Corporation is presently using a computer with a repetition rate of 3500 iterations/sec. This will be replaced shortly by a new microprocessor with a 15,000 iterations/sec capability.

EA-81, 843

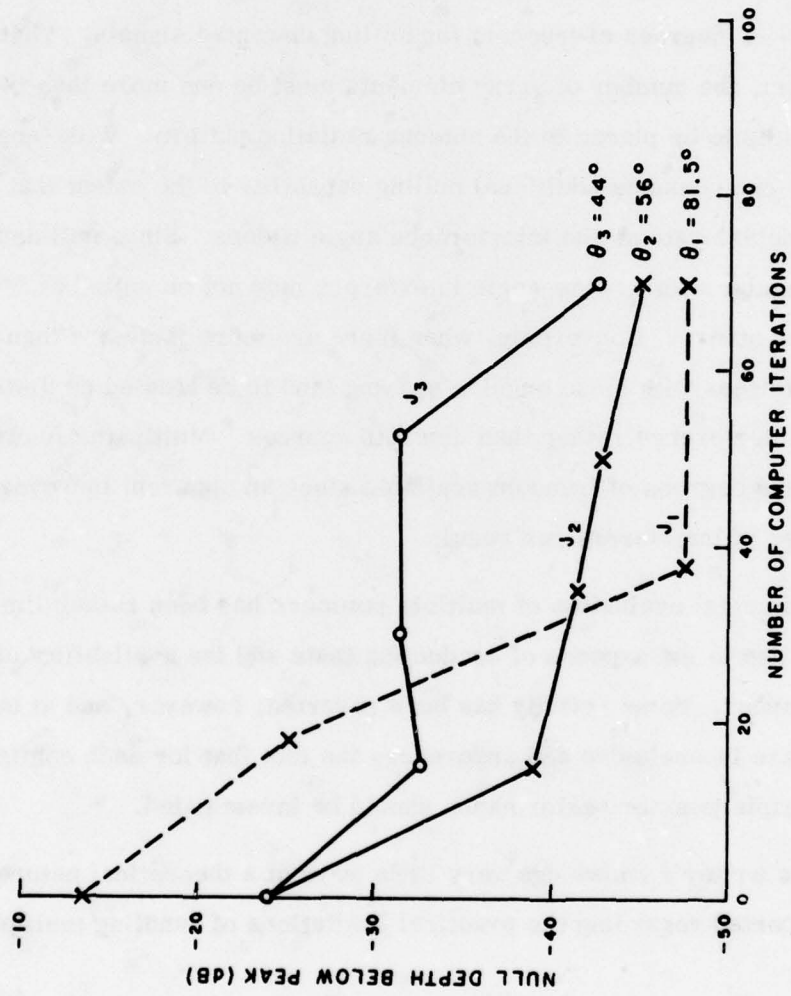


Figure A.6 Convergence Response

A.4.3 Number of Nulls

In general an adaptive array antenna containing N elements has no more than $N - 1$ degrees of freedom for nulling unwanted signals. That is, as a minimum, the number of array elements must be one more than the number of nulls to be placed in the antenna radiation pattern. Wide-angle interference can consume additional nulling capability to the extent that null depths will deteriorate as the interference angle widens. Since null depths vary with angular width, wide-angle interferers may not be nulled as effectively as others. Conversely, when there are more jammers than array elements, sources with close angular spacing tend to be treated as distributed wide-angle interference rather than discrete sources. Multipath effects can reduce the degrees of freedom available since an apparent increase in the number of interferers can result.

Experimental evaluation of multiple jammers has been rather limited, presumably due to the expense of conducting tests and the availability of jamming sources. Some activity has been reported, however, and at best the results are inconclusive and underscore the fact that for each configuration the multiple jammer performance should be investigated.

To this writer's knowledge very little work of a theoretical nature has been reported regarding the practical limitations of handling multiple interferers.

Baird et al., (15) have reported several simulation results (figures A.7, A.8, and A.9) that seem to underline the unknown nature of the multiple jammer situation. In the curves M is the number of array elements, BW is fractional bandwidth, and jammer/signal = 30 dB. Jamming signals are added sequentially starting with a single jammer and increasing in some cases beyond $N - 1$. In one interferer location configuration (figure A.7),

IA-51,540

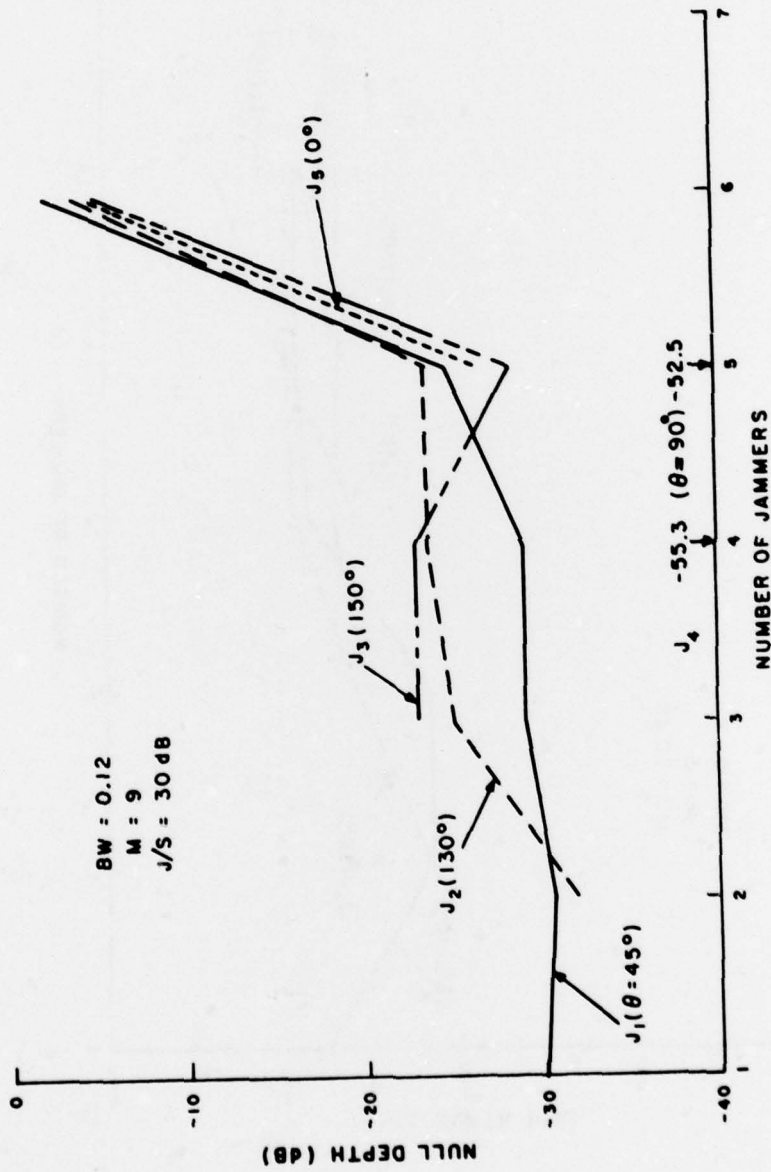


Figure A.7 Multiple Jammer Performance

IA-31, 841

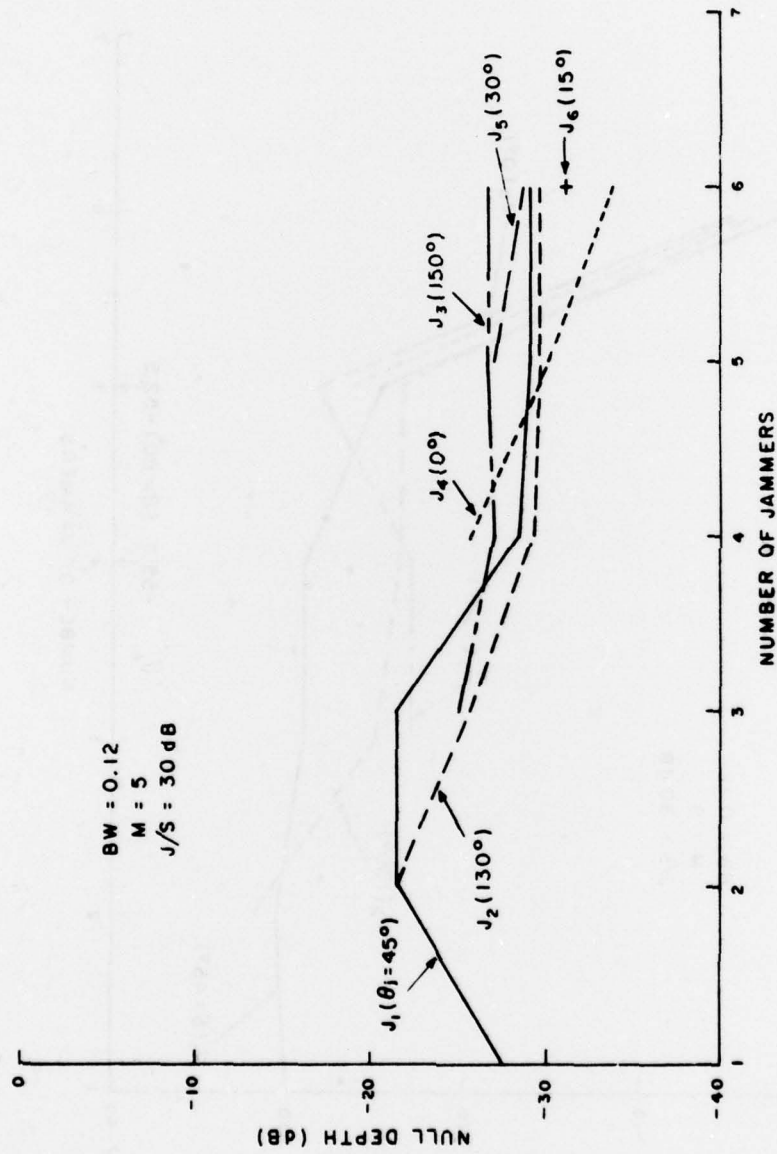


Figure A.8 Multiple Jammer Performance

IA-31,942

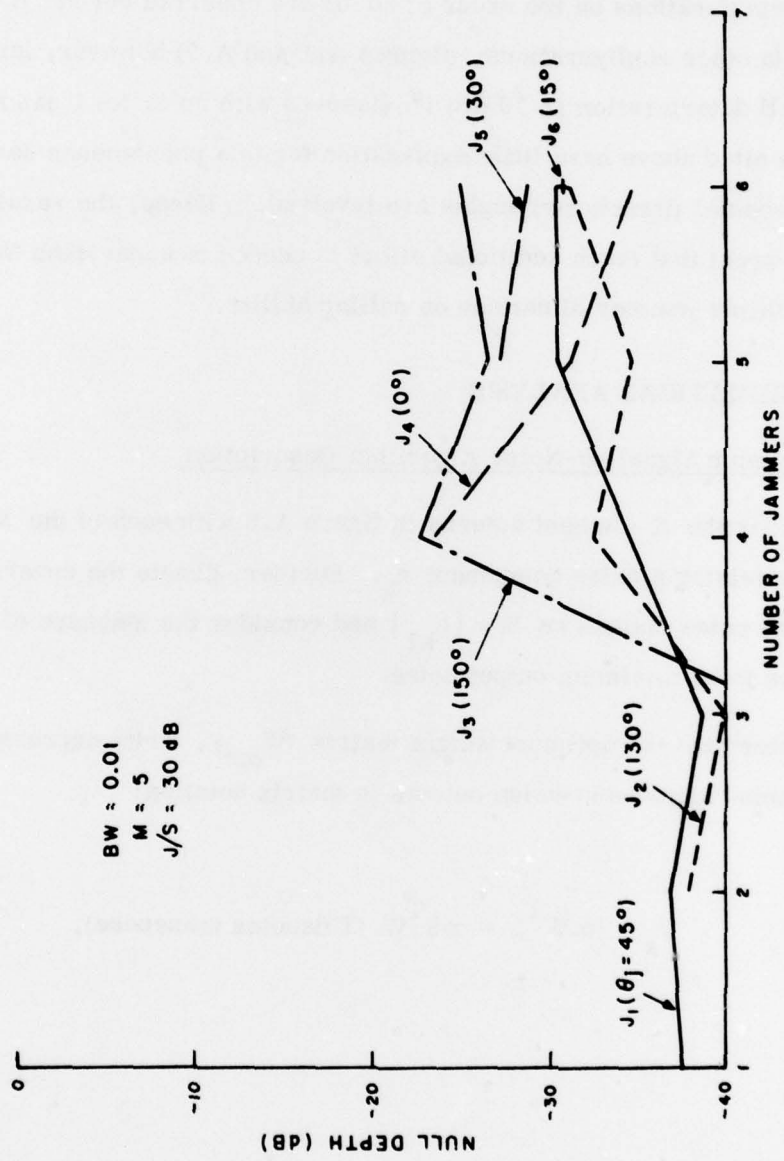


Figure A.9 Multiple Jammer Performance

null depth deteriorations on the order of 20 dB are observed beyond $N - 4$ jammers. In other configurations, (figures A.8 and A.9) however, less dramatic null deterioration (~ 10 dB) is observed with up to $N + 1$ jammers. The authors cited above have little explanation for this phenomenon save to state that "special (interferer) angles are involved." Hence, the results are further proof that much additional effort is needed to understand the effect of multiple jammer situations on nulling ability.

A.5 MATHEMATICAL ANALYSIS

A.5.1 Maximum Signal-to-Noise Algorithm Description

Consider the K element antenna in figure A.3 with each of the K channels containing a noise component n_k . Further, denote the covariance* matrix of the noise outputs as $M = [\mu_{k1}]$ and consider the measure of performance to be minimum output noise.

To determine the optimum weight matrix (W_{opt}), write expressions for the summed signal-and-noise outputs in matrix notation:

Signal

$$V_s = \alpha W^T S = \alpha S^T W \text{ (T denotes transpose),}$$

*The covariance of two random variables x and y is equal to $E(x - \mu_x)(y - \mu_y)$ where μ_x denotes the expected value or mean of x and μ_y is the expected value of y .

where

$$\alpha S = \alpha \begin{bmatrix} S_1 \\ S_2 \\ \vdots \\ S_k \end{bmatrix}$$

and represents the signal in the K channels, and noise $V_n = W^T N$, where

$$N = \begin{bmatrix} n_1 \\ n_2 \\ \vdots \\ n_k \end{bmatrix} .$$

The mean square or expected value (E) of the output noise power is:

$$\begin{aligned} P_n &= E \left\{ |V_n|^2 \right\} = E \left\{ |W^T N|^2 \right\} \\ &= E \left\{ (W^T N)^* (N^T W) \right\} \\ &= E \left\{ W^{T*} N^* N^T W \right\} . \end{aligned}$$

Since only the noise terms are being averaged

$$P_n = W^{T*} E \left\{ N^* N^T \right\} W ,$$

where $E \left\{ N^* N^T \right\} = M = [\mu_{k1}]$ is the covariance matrix of the input noise terms, and $P_n = W^{T*} N W$.

For the noise components to be uncorrelated, M must be diagonalized. If the noise element in each channel is denoted by n_k , the covariance of n_k and the noise in another channel n_1 is $\mu_{k1} = E(n_k^* n_1)$. Since $\mu_{1k} = E(n_1^* n_k) = \mu_{k1}^*$ the matrix is Hermitian positive definite. For a positive definite Hermitian matrix there exists a transformation matrix that diagonalized the

matrix M thereby delivering the problem as one in which all channels have equal uncorrelated noise power components.

It can be shown (16) that when the noise elements are of equal powers and uncorrelated, the optimum weight vector $(\hat{W}_{opt}) = \mu S^*$ (where the caret (\wedge) denotes posttransformation quantities) and μ is a constant.

Applebaum goes on to show that the optimum weight vector for the combiner is

$$W_{opt} \hat{=} \mu M^{-1} S^*$$

and that this optimum weight yields the optimum signal-to-noise ratio.

$$(S/N)_{opt} = \left| \infty \right|^2 S_t M^{-1} S^*$$

We note that mathematically the optimum weight vector is proportional to the inverse of the covariance matrix (M) of the noise outputs.

A.5.2 Least Mean Square (LMS) Error Algorithm

Consider the receive antenna system shown in figure A.4, where the output of each element is denoted by $e(t)$. The element signals are summed to produce an array output $S(t)$. Classically, the array is made adaptive by comparing the output $S(t)$ to some reference signal $R(t)$. The difference or error signal $e_o(t)$ provides the input to a feedback system, which in turn controls the complex element weights W_k . In the system under discussion the feedback is designed to adjust the weights to minimize the mean square value of $e_o(t)$. Hence the output signal $S(t)$ is forced to approximate the reference signal on a mean square basis. Any received signal not represented in $R(t)$ contributes to the error signal. The weights are appropriately adjusted by the feedback and the signal is removed from the output. Thus the antenna collecting aperture effectively contains a null in the direction of this undesired signal.

The complex element weights can be implemented through utilization of quadrature hybrids and variable attenuators. Each element signal is divided into in-phase and quadrature components and multiplied by a weight W_k .

$$S(t) = W^T x(t), \quad (1)$$

where W^T is the transpose of the weight vector

$$W = \begin{bmatrix} W_1 \\ W_2 \\ \downarrow \\ W \end{bmatrix} \quad (2)$$

and

$$x(t) = \begin{bmatrix} x_1(t) \\ x_2(t) \\ \downarrow \\ x_k(t) \end{bmatrix} \quad (3)$$

is the signal input vector.

The error signal is the difference between the wanted response $R(t)$ and the output response $W^T x(t)$:

$$e_o(t) = R(t) - W^T x(t). \quad (4)$$

Squaring:

$$e_o^2(t) = R^2(t) + W^T x(t)x(t)^T W - 2R(t)W^T x(t). \quad (5)$$

Then the expected value of the square error or the mean square error is

$$\begin{aligned} E[e_o^2(t)] &= E[R(t)^2 + W^T x(t)x(t)^T W - 2R(t)W^T x(t)] \\ &= E[R^2] + W^T \phi(x, x) W - 2W^T \phi(x, R). \end{aligned} \quad (6)$$

In more convenient form

$$E[e_o^2(t)] = E[R^2] - 2W^T S + W^T \phi W. \quad (7)$$

In equation (7), S is a column matrix representing a set of cross-correlations between the k input signals and the desired output response signal as follows:

$$S = \phi(x, R) = E(x, R) = E \begin{bmatrix} x_1 R \\ x_2 R \\ \vdots \\ x_k R \end{bmatrix}, \quad (8)$$

where ϕ is a matrix of cross-correlations and auto-correlations of input signals to the adaptive element

$$\phi = \phi(x, x) = E(x, x^T) = E \begin{bmatrix} x_1 x_1 & x_1 x_2 & x_1 x_n \\ x_2 x_2 & & \\ x_n x_1 & & x_n x_n \end{bmatrix}. \quad (9)$$

The mean square error defined in equation (6) is a quadratic function of the weights and hence has a well-defined minimum. This function can be thought of as an inverted three-dimensional bell-shaped curve. To yield the gradient*, $\nabla E[e_o^2]$ of the function, equation (6) is differentiated with respect to W and

$$\nabla E[e_o^2] = 2\phi(x, x)W - 2\phi(x, R). \quad (10)$$

To optimize the weights, the gradient of the surface must be zero and it can be shown that:

$$\begin{aligned} 2\phi(x, x)W_{\text{opt}} - 2\phi(x, R) &= 0, \\ \phi(x, x)W_{\text{opt}} &= \phi(x, R), \\ W_{\text{opt}} &= \phi^{-1}(x, x)\phi(x, R). \end{aligned} \quad (11)$$

Note that the optimum solution calls for inversion of the matrix of the correlations of input signals to adaptive element. It turns out that for large arrays, the solution to equation (11) presents formidable computational problems since it calls for the inversion of an $n \times n$ matrix and repeated updates of estimates of the elements of the correlation matrices. Therefore, approximate methods are used to find solutions to the optimum weight equation. One such method is based on the method of steepest descent and is called the LMS algorithm.

*The gradient of a surface (in this case that formed by $e_o^2(t)$ versus the element weights) is a vector in the direction of maximum space rate of change.

Changes to the weight vector are made along the gradient vector and, accordingly, the weight after adaptation or weight iteration is:

$$W(t+1) = W(t) + k_s \hat{\nabla}(t),$$

where

$W(t)$ is the weight vector at the sampling instant t prior to adaptation,

k_s is a scalar constant related to the convergence and stability of the algorithm,

$\hat{\nabla}(t)$ is estimated gradient vector of the mean square error function $E[e_o^2]$ with respect to W .

To obtain the estimated gradient of the mean square error, we take the gradient of a single time sample of the square error

$$\nabla[e_o^2(t)] = 2e_o(t) \nabla[e_o(t)].$$

From previous discussion, the error signal $e_o(t) = R(t) - W^T x(t)$.

Therefore, the gradient of $e_o(t)$ with respect to W is

$$\begin{aligned} \nabla[e_o(t)] &= \nabla[R(t) - W^T(t)x(t)] \\ &= -x(t) \end{aligned}$$

and

$$\hat{\nabla}(t) = -2e_o(t)x(t).$$

The weight iteration formula becomes

$$W(t+1) = W(t) - 2k_s e_o(t)x(t).$$

This indicates that successive weight vectors are derived by adding the input vector scaled by the error value to the present weight. Since the gradient measures the slope of $e_o^2(t)$ with respect to each of the weights, the weight iteration formula states that a given weight will be changed at a rate proportional to the sensitivity of the $e_o^2(t)$ surface to that weight, i.e., the absolute slope of the surface curve decreases as the surface minimum is approached.

It is clear that the choice of k_s is critical to the performance of this algorithm. If k_s is too large, the corrections $k_s \nabla(t)$ will be so large that the updated values will oscillate on each side of the minimum. If, on the other hand, k_s is too small, the approximation will converge too slowly. It is also apparent that the gradient becomes small and approaches zero as the minimum is reached; hence the convergence rate slows or optimization is near.

REFERENCES

1. Y. Okumura, et al., "Field Strength and Its Variability in VHF and UHF Land-Mobile Radio Service," Review Tokyo Elec. Comm. Lab., Vol. 16 (Sept.-Oct. 1968), pp. 825-873. Reprinted in Communications Channels: Characterization and Behavior, B. Goldberg, ed., New York: IEEE Press, 1976.
2. W. Rotman and R.F. Turner, "Wide-Angle Microwave Lens for Line Source Applications," IEEE Transactions on Antennas and Propagation, November 1963, pp. 623-632.
3. S.S.D. Jones, H. Gent, and A.A.L. Browne, "Improvements in, or Relating to, Electromagnetic-Wave Lens and Mirror Systems," British Provisional Patent Specification No. 25926/56; August 1956.
4. N. Abramson, "The Aloha System," Chapter 14 in Computer Communication Networks, N. Abramson and F.F. Kuo, eds., Englewood Cliffs, N.J.: Prentice-Hall, 1973.
5. I.G. Stiglitz, "Multiple Access Considerations - A Satellite Example," IEEE Transactions on Communications, Vol. COM-21 (May 1973), pp. 572-582.
6. S.A. Reible, J.H. Cafarella, R.W. Ralston, and E. Stern, "Convolver, for DPSK Demodulation of Spread Spectrum Signals," 1976 Ultrasonics Symposium Proceedings, pp. 451-455.
7. J.M. Wozencraft and I.M. Jacobs, Principles of Communication Engineering, New York: Wiley, 1965.
8. Paul Baran, "On Distributed Communication Networks," IEEE Trans., Vol. CS-12 (March 1964), pp. 1-9.
9. B.W. Boehm and R.L. Wobley, "Adaptive Routing Techniques for Distributed Communications Systems," IEEE Trans., Vol. COM-17 (June 1969), pp. 340-349.
10. B. Widrow, P.E. Mantey, L.J. Griffiths, B.B. Goode, "Adaptive Antenna Systems," Proc. IEEE, Vol. 55, No. 12 (December 1967).
11. S.P. Applebaum, "Adaptive Arrays," IEEE Trans. on Antennas and Propagation, Vol. AP-24, No. 5 (September 1976).
12. J.S. Reed, J.D. Mallett, L.E. Brennan, "Rapid Convergence Rate in Adaptive Arrays," IEEE Trans. on Aerospace and Electronic Systems, Vol. AES-10, No. 6 (November 1974).

REFERENCES (Concluded)

13. Private conversation with L. Horowitz, MIT Lincoln Lab.
14. B.S. Abrams, et al., "Interference Cancellation," General Atronics Corp., RADC TR-74-226, September 1974.
15. C.A. Baird, G.G. Rassweiler, C.L. Zahm, G.P. Martin, Radiation Inc., RADC TR-72-174, July 1972.
16. W.F. Gabriel, "Adaptive Arrays - An Introduction," Proc. IEEE, Vol. 64, No. 2 (February 1976).
17. L.E. Brennan, E.L. Pugh, I.S. Reed, "Control-Loop Noise in Adaptive Array Antennas," IEEE Trans. on Aerospace and Electronic Systems, Vol. AES 7, No. 2 (March 1971).
18. G. Rassweiler, A. Roy, C. Baird, D. Lehman, "Digitally Controlled Adaptive Array for RPV Multiple Beam Antenna System," Harris Corp. (RADC, USAF Avionics Lab.); Proc. Adaptive Antenna Systems Workshop, Vol. I (September 1974).